Check for
updates

Impact of Earth's Mean Time-Variable Gravity Field Models on Precise Orbits of Altimetry Satellites

Sergei Rudenko[1,2] · Denise Dettmering[1] · Jean-Michel Lemoine[3] · Mathis Bloßfeld[1] · Julian Zeitlhöfler[1]

Abstract

Gravitational forces are the major forces acting on near-Earth orbiting (e.g., altimetry) satellites. We perform a review of Earth's mean time-variable gravity (TVG) field models developed in the past 23 years (2000–2023). This includes the models developed using CHAMP, GRACE, GRACE-FO, GOCE, SLR (Satellite Laser Ranging), and DORIS measurements. Some of these models contain just secular terms, while more recent models include also periodic (annual and semi-annual) variations of the Earth's gravity. We show the impact of these models on precise orbit determination (POD) of selected altimetry satellites, namely TOPEX/Poseidon, Jason-1, Jason-2, and Jason-3 at the time interval from 1992 to 2023. The impact of these models is assessed for different orbit parameters as well as the root-mean-square (RMS) and mean values of SLR observation residuals and orbit differences. Furthermore, the impact of these models on altimetry (single- and multi-satellite) sea surface height crossover differences, radial errors, geographically correlated mean errors, and their trends is analyzed. We have found that the CNES RL05MF model derived using data of 1985–2022 performs best among the models tested in this study, particularly for the Jason-3 time span (2016–2023). Using this model reduces the RMS values of SLR observation residuals from 2.56 cm (for pre-CHAMP model GRIM5-C1) to 1.48 cm for this satellite. The RMS values of orbit differences in the radial direction fit within 0.7–0.8 cm for most recent TVG models, while using old GRIM5-C1 would result in 1.9 cm differences. It is important to reprocess regularly Earth's TVG data covering the longest time span to minimize extrapolation errors of the models.

1 Introduction

Global, regional, and coastal sea levels are among the key indicators of climate change (Sandford et al. 2024). The Global Mean Sea Level (GMSL) rise is caused mainly by the ocean thermal expansion and meltwater from melting glaciers and land-based ice sheets due to global warming (Cazenave and Moreira 2022). The average GMSL rate is

3.3±0.3 mm/year over the time span from 1993 through 2023, and its acceleration counts 0.08±0.06 mm/year², so that the GMSL rate has doubled since the beginning of the satellite radar altimetry era reaching 4.5–4.8 mm/year between 2014 and 2023, as compared to 2.1–2.3 mm/year between 1993 and 2002 (Cazenave and Moreira 2022; Hamlington et al. 2024; World Meteorological Organization State of the Global Climate 2023). The 2022 Global Climate Observing System (GCOS) Essential Climate Variables (ECVs) Requirements establish a 0.3 mm/year requirement for the regional mean sea level trend determination (GCOS 2022). Since sea surface height is determined in satellite radar altimetry referred to the position of the satellite-based radar altimeter with respect to reference ellipsoid, this requires centimeter and even sub-centimeter accuracy of satellite position in space (International Altimetry Team 2021). Though the accuracy of altimetry satellite orbits improved significantly in the last decades (Rudenko et al. 2023), orbit errors still remain to be the main contributor to the errors of regional sea level rise and its variability (Meyssignac et al. 2023).

Several studies were performed in the recent years to quantify the impact of orbit errors on the mean sea level trend at regional scale. Thus, Ablain et al. (2017) estimated the trend uncertainty of the order of 2–3 mm/year at this scale. They stress that although the orbit error was significantly reduced for this spatial scale during the recent decade, it remained the main source of uncertainty (in the range of 1–2 mm/year; (Couhert et al. 2015)) at that time. The major contributions to remaining orbit errors are remaining errors of Earth's gravity field models and terrestrial reference frames, in which orbits are computed (Couhert et al. 2015; Rudenko et al. 2023). The Earth's gravity field model errors explained a significant part of these uncertainties (Rudenko et al. 2014). From the comparison of orbits of altimetry satellites TOPEX/Poseidon, Jason-1, and Jason-2 computed using Doppler Orbitography and Radiopositioning Integrated by Satellite (DORIS) and Satellite Laser Ranging (SLR) measurements in ITRF2008 and ITRF2014, Zelensky et al. (2018) found that the radial orbit drifts reach ±0.2 mm/year on a regional scale. Rudenko et al. (2019) obtained changes up to 0.4 mm/year in the regional sea level trend on interannual timescales (3–8 years) in the time span from April 1993 to July 2008 and up to 1.0 mm/year in the time span from July 2008 to April 2015, when analyzing DORIS and SLR observations-based orbits, while switching from ITRF2008 to ITRF2014. Comparisons between altimetry products computed using two different orbit solutions (POE-D and POE-E) exhibit trend differences below 1 mm/year regionally (Prandi et al. 2021).

Gravitational forces are the major forces acting on near-Earth orbiting satellites. Accurate modeling of the Earth's gravity field is very important for precise orbit determination (POD) of Low Earth Orbit (LEO) and, in particular, altimetry satellites. CHAMP (CHAllenging Minisatellite Payload) was the first LEO satellite dedicated to Earth's gravity field determination equipped with a Global Positioning System (GPS) receiver and an accelerometer on board to measure in situ the surface forces acting on the satellite (Reigber et al. 2003). Recently published Earth's gravity field models used for the satellite POD have been derived based on observations of GRACE (Gravity Recovery And Climate Experiment, Tapley et al. 2004) and GRACE-FO (GRACE Follow-On, Landerer et al. 2020) gravity field satellite missions between 2002 and 2017 and since 2018, respectively. A comprehensive review of the gravimetric missions CHAMP, GRACE, and GOCE (Gravity and steady-state Ocean Circulation Explorer, Drinkwater et al. 2003) and gravity field models derived from their measurements is done by Flechtner et al. (2021). Analysis of the measurements of the GRACE and GRACE Follow-On missions allowed to derive Earth's time-variable gravity field models (abbreviated hereafter as "TVG models"). Ollivier et al. (2012) and Rudenko et al. (2014) showed the importance of modeling time-variability of

the Earth's gravity field in POD of altimetry satellite. They found that ignoring this variability leads to the errors of up to 3 mm/year in regional sea level trends that are 10 times larger than the requirement of the GCOS for the determination of the regional mean sea level trend.

There are different ways of representing Earth's time-variable gravity. One of them, being most commonly used in the POD of altimetry and other Earth orbiting satellites, are mean gravity field models, in which coefficients of the spherical harmonic expansion of the Earth's geopotential are given as a formula (c.f. Eq. 1) providing static and time-variable parts of the model. TVG models described in Sect. 2 belong to this type. Another way of representing the Earth's gravity field variations is using point mass concentrations (mascons, see, e.g., Cerri et al. 2013). A third way is using gravity field solutions for dedicated time periods. They are provided usually in the form of monthly geopotential spherical harmonics. Such solutions are available from the Center for Space Research (CSR) at University of Texas, Austin, Helmholtz Centre Potsdam German Research Centre for Geosciences (GFZ), and Jet Propulsion Laboratory (JPL) and at the International Centre for Global Earth Models (ICGEM, Ince et al. 2019) web page.[1] Gruber et al. (2018) obtained comparable results in the POD of altimetry satellites Envisat, Jason-1, and Jason-2, when using GRACE TVG field solutions (GFZ RL05a) and Earth's mean gravity field model EIGEN-6S4 (Förste et al. 2016). EIGEN stands for "European Improved Gravity model of the Earth by New techniques". A series of EIGEN models were jointly developed by GFZ and Groupe de Recherches de Géodésie Spatiale (GRGS) Toulouse. A disadvantage of using monthly geopotential solutions are the gaps, in which no solution is available for some months. The gaps were especially frequent at the end of the GRACE mission in 2015–2017. A few approaches have been developed recently to fill in data gaps within the GRACE mission data. One of them is an approach composed of the Singular Spectrum Analysis gap-filling technique, cross-validation, and spectral testing for significant components (Yi and Sneeuw 2021). Weigelt et al. (2024) suggested to use high-low satellite-to-satellite tracking data derived from GPS measurements to LEO satellites in combination with SLR observations of spherical geodetic satellites. Finally, Schrama and Visser (2024) proposed to use Fourier approximation of the TVG at the gaps.

Additionally, using SLR measurements of spherical geodetic satellites allows to determine spherical harmonic coefficients of the Earth's gravity field expansion of low degree and order (d/o) more precisely than using just GRACE/GRACE-FO data (see, e.g., Cheng and Ries (2023)). It should be mentioned that the TVG information is inhomogeneous over the time interval 1985–2023, since different data were used at different time intervals. Therefore, the quality of the TVG models based on this information is not homogeneous.

In this paper, we perform a review of Earth's mean TVG models developed in 2000–2023 and show the impact of some of these models on POD of altimetry satellites and altimetry results obtained from the analysis of satellite orbits based on these models. Namely, we investigate the impact of nine selected Earth's mean TVG models on POD of four altimetry satellites: TOPEX/Poseidon (1992–2005), Jason-1 (2002–2013), Jason-2 (2008–2019), and Jason-3 (2016–2023) at the time spans given. We consider in this study these so-called altimetry reference missions for the period from 1992 to 2023. They have the same 9.92-day orbital cycle at high altitude (1336 km) and are used for the long-term stability and investigations of large-scale changes of global sea level products (Legeais,

---

[1] https://icgem.gfz-potsdam.de/sl/temporal

et al., 2018). We search for an Earth's mean TVG model that performs best over the complete 31-year time span (1992–2023). Then we quantify orbit errors in the radial direction for the cases, when other Earth's mean TVG models are used, as compared to the best quality model. Using different models for various satellites and time spans might introduce artificial orbit errors that may map into altimetry products. We have selected mean gravity field models of releases 2–5 developed at Centre National d'Etudes Spatiales (CNES)/GRGS, as well as Earth's TVG models developed since 2000 and available at the ICGEM web page.[2] These are GRIM5-C1 model developed in 2000 before the launch of CHAMP and GRACE, EIGEN-GL04S1 (Förste et al. 2008b) model based on GRACE data from February 2003 to July 2005, EIGEN-6S (Förste et al. 2011), GOCO06S (Kvas et al. 2021) being the latest version of the Gravity Observation Combination (GOCO) consortium global gravity field models, as well as ITSG-GRACE2018S (Kvas et al. 2019) being the latest GRACE-only gravity field model computed at the Institute of Geodesy of the Graz University of Technology.

We show the impact of the Earth's gravity field models on the following parameters:

- root-mean-square (RMS) and mean values of SLR observation residuals,
- orbit differences in the radial direction being the most important direction for altimetry satellites, since any mismodeling in this direction will map in the sea surface height computed from the radar altimetry measurements and, as a result, in sea level and its trend, if this mismodeling is systematic,
- scale factors of the solar radiation pressure, Earth's albedo and infrared radiation, and atmospheric drag,
- sine and cosine terms as well as coefficients of a continuous piecewise linear function of the along-track and cross-track empirical accelerations.

Furthermore, the impact of these models on altimetry (single- and multi-satellite) sea surface height crossover differences is investigated. From these crossover differences, radial errors and geographically correlated mean errors are derived and analyzed.

This paper is organized as follows. Section 2 describes the Earth's mean TVG models developed in 2000–2023. A description of POD and the models and corrections used is provided in Sect. 3. Section 4 provides the results of the impact of the gravity field models on the orbital parameters and orbit differences, while Sect. 5 presents the altimetry crossover results. Conclusions are given in Sect. 6.

2 Earth's Mean Time-Variable Gravity Field Models

A general formula for the computation of a spherical harmonic coefficient $\bar{C}_{nm}$ of degree n and order m at the time instant t is as follows, where the time-variable part of the model consists of a trend, sine and cosine terms of annual and semi-annual variations of each spherical harmonic coefficient up to a given d/o:

---

[2] https://icgem.gfz-potsdam.de/home

Table 1 Earth's mean gravity field models containing secular terms, but no periodic variations of geopotential coefficients. The models are sorted chronologically by the year of their publication

Model name	Year	Data time span	Max. degree of the static part	Secular terms (degree of zonal terms)	References
GRIM5-S1	2000	1971–1998	99	2–4	Biancale et al. (2000)
GRIM5-C1	2000	1971–1998, 2000	120	2–4	Gruber et al. (2000)
TEG4	2000	2000	200	2 and (2,1)	Tapley et al. (2000)
EIGEN-1s	2002	2000	119	2–4	Reigber et al. (2002)
EIGEN-CHAMP03Sp	2003	Jul. 2000–Jun. 2003	140	2–4	Reigber et al. (2005a)
EIGEN-CHAMP03S	2004	Oct. 2000–Jun. 2003	140	2–4	Reigber et al. (2005a)
EIGEN-GRACE02S	2004	2002–2003 (5 months)	150	2–4	Reigber et al. (2005b)
GGM02S	2004	Apr. 2002–Dec. 2003	160	2	Tapley et al. (2005)
GGM02C	2004	Apr. 2002–Dec. 2003	200	2	Tapley et al. (2005)
EIGEN-CG01C	2004	Oct. 2000–Nov. 2003	360	2–4	Reigber et al. (2006)
EIGEN-CG03C	2005	Oct. 2000–Jul. 2004	360	2–4	Förste et al. (2005)
EIGEN-GL04S1	2006	Feb. 2003–Jul. 2005	150	2–4	Förste et al. (2008b)
EIGEN-GL04C	2006	Feb. 2003–Jul. 2005	360	2–4	Förste et al. (2008b)
EIGEN-5S	2008	Jan. 2001–Jan. 2007	150	2–4 and (2,1)[a]	Förste et al. (2008a)
EIGEN-5C	2008	Jan. 2001–Jan. 2007	360	2–4 and (2,1)[a]	Förste et al. (2008a)
EIGEN-CHAMP05S	2010	Oct. 2002–Sep. 2008	150	2–4 and (2,1)[a]	Flechtner et al. (2010)
EIGEN-51C	2010	Oct. 2002–Sep. 2008	359	2–4 and (2,1)[a]	Bruinsma et al. (2010)
AIUB-GRACE03S	2011	Jul. 2003–Aug. 2009	160	2–30[b]	Jäggi et al. (2011)

[a]Also for this tesseral term. [b]For all terms of the given range

$$
\begin{aligned}
\bar{C}_{nm}(t) = {} & \bar{C}_{nm}^0 + \dot{\bar{C}}_{nm}\Delta t_e + \bar{C}_{nm}^{\mathrm{SINA}} \sin(2\pi\Delta t_p) + \bar{C}_{nm}^{\mathrm{COSA}} \cos(2\pi\Delta t_p) \\
& + \bar{C}_{nm}^{\mathrm{SINS}} \sin(2 \cdot 2\pi\Delta t_p) + \bar{C}_{nm}^{\mathrm{COSS}} \cos(2 \cdot 2\pi\Delta t_p)
\end{aligned}
\tag{1}
$$

where $\bar{C}_{nm}^0$ is the spherical harmonic coefficient at the reference epoch t_{epoch} (a static part), $\Delta t_e = t - t_{\mathrm{epoch}}$, in years of 365.25 days, t_{epoch} is the reference epoch given with the bias coefficient (in days), $\dot{\bar{C}}_{nm}$ means a time derivative of $\bar{C}_{nm}$ (a secular term), $\Delta t_p = t - $ 1st of January of the given year, in years of 365.25 days, $\bar{C}_{nm}^{\mathrm{SINA}}$, $\bar{C}_{nm}^{\mathrm{COSA}}$, $\bar{C}_{nm}^{\mathrm{SINS}}$, and $\bar{C}_{nm}^{\mathrm{COSS}}$ are the

amplitudes of the sine and cosine terms of annual and semi-annual (periodical) variations of the spherical harmonic coefficient, respectively. The degree 0 term in Eq. 1 corresponds to the point-like attraction and is equal to 1. The degree 1 terms are put to 0 in orbit tests described in Sects. 3–5, thus identifying the center of mass of the Earth with the origin of the terrestrial reference frame.

2.1 Earth's Gravity Field Models Containing Just Secular Terms

A list of Earth's gravity field models containing secular terms, but no periodic variations of geopotential coefficients is given in Table 1. From these models, GGM02S (Tapley et al. 2005) and GGM02C (Tapley et al. 2005) contain secular terms of zonal coefficients just of degree 2. TEG4 (Tapley et al. 2000) contains additionally secular term of the coefficient (2,1). Other models given in this table contain secular terms for zonal coefficients of degrees 2–4, while EIGEN-5C, EIGEN-5S (Förste et al. 2008a), EIGEN-CHAMP05S (Flechtner et al. 2010), and EIGEN-51C (Bruinsma et al. 2010) contain secular terms also of the coefficients (2,1), and AIUB-GRACE03S (Jäggi et al. 2011) contains secular terms of d/o 2–30. The satellite-only model GRIM5-S1 (Biancale et al. 2000) and combined model GRIM5-C1 (Gruber et al. 2000) were developed before the CHAMP launch (in 2000) using tracking data to 21 satellites over the time span 1971–1998 and additionally of 2000, as well as terrestrial and altimetric gravity anomaly data, in case of GRIM5-C1. The static part of these two models contains coefficients up to d/o 99 and 120, respectively. These models served as reference gravity field models for CHAMP initial processing. EIGEN-1s (Reigber et al. 2002) was the first model based on CHAMP data, namely on 88 days of year 2000. Geoid approximation error of this model was of about 20 cm in terms of $5° \times 5°$ block mean values (Reigber et al. 2002). The EIGEN-CHAMP03Sp (Reigber et al. 2005a) and EIGEN-CHAMP03S (Reigber et al. 2005a) were derived from GPS-CHAMP satellite-to-satellite tracking and accelerometer data covering about a 2.5-year time span in 2000–2003 and SLR data of four satellites. These models revealed large-scale temporal gravity field variations due to sub-seasonal and seasonal mass variations in the atmosphere, oceans and continental hydrology (Reigber et al. 2005a). These models are complete up to d/o 140. EIGEN-GRACE02S (Reigber et al. 2005b) was the first Earth's gravity field model calculated from GRACE tracking data, namely 110 days in 2002–2003. Dedicated instrumentation of GRACE mission (a K-band ranging assembly, an accelerometer, a GPS receiver, a star camera and other instruments) allowed to derive an Earth's gravity field model being about one order of magnitude more accurate than CHAMP-derived global gravity field models and over two orders of magnitude more accurate than the pre-CHAMP satellite-only gravity field models of that time (Reigber et al. 2005b). The satellite-only model GGM02S and combined model GGM02C were calculated from 14 months of data (April 2002–December 2003) of GRACE measurements indicating a cumulative error of less than 1 cm geoid height to spherical harmonic degree 70 (Tapley et al. 2005). From the combination of GPS-CHAMP and GPS-GRACE high-low and GRACE K-band range low-low satellite-to-satellite tracking data at the about three-year time interval from October 2000 to November 2003 as well as surface data from altimetry over the oceans and gravimetry over the continents, a new, high-resolution global gravity field model EIGEN-CG01C (Reigber et al. 2006) was determined. This model had the accuracy of 4 cm and 0.5 mgal in terms of geoid heights and gravity anomalies, respectively, at a spatial resolution of 200 km half-wavelength. EIGEN-CG03C (Förste et al. 2005) was an upgrade to EIGEN-CG01C based on the same CHAMP data, but almost

twice as much GRACE data (376 days instead of 200 days, totally from October 2000 until July 2004), Förste et al. (2005). Both EIGEN-CG01C and EIGEN-CG03C are complete up to d/o 360. EIGEN-CG03C was selected as a reference Earth's gravity field model of the Geophysical Data Records (GDR) orbit standards (version B: GDR-B[3]). EIGEN-GL04S1 (Förste et al. 2008b) is a satellite-only model based on 30 months of GRACE data covering the period from February 2003 until July 2005. Additionally, 24 months (February 2003 to February 2005) of LAGEOS SLR data were used for accurate estimation of $C_{2,0}$. EIGEN-GL04C (Förste et al. 2008b) is a combined model computed using the same data as EIGEN-GL04S1, but additionally surface gravity data sets in the Arctic, Antarctic, and North America, and a new mean sea surface height model from altimetry processing at GFZ. The accuracy of this model at a spatial resolution of 200 km (half-wavelength) was 3 cm in terms of geoid heights. EIGEN-GL04S1 and EIGEN-GL04C are complete up to d/o 150 and 360, respectively. Satellite-only model EIGEN-5S (Förste et al. 2008a) was derived using 54 months (August 2002–January 2007) of GRACE data and 6 years (January 2001 – December 2006) of LAGEOS-1/-2 SLR data. A new combined gravity field model EIGEN-5C (Förste et al. 2008a) was obtained from the combination of these data with surface data. This model showed better performance compared to previously released models, in particular, smaller observation fits for GRACE and SLR satellites, smoother spectral behavior, better reduction of meridional stripes and smaller fit in GPS/leveling comparisons (Förste et al. 2008a). EIGEN-5S and EIGEN-5C were complete up to d/o 150 and 360, respectively. EIGEN-CHAMP05S gravity field model was computed using six years (October 2002–September 2008) of reprocessed CHAMP GPS-SST and accelerometer data (Flechtner et al. 2010). The maximum d/o of this gravity field model is 150. This model indicated better quality than its predecessor EIGEN-CHAMP03S also based on CHAMP data. This was obtained due to using a longer time span of data, application of improved background modeling, processing standards and strategies. At the same time, EIGEN-CHAMP05S showed comparable quality as, e.g., EIGEN-5S derived using GRACE data. EIGEN-51C is a combined global gravity field model derived using six years of CHAMP and GRACE data (from October 2002 to September 2008) and the DNSC08 global gravity anomaly data set (Bruinsma et al. 2010). The model is complete up to d/o 359. Finally, AIUB-GRACE03S is a GRACE-only gravity field model computed using GRACE GPS satellite-to-satellite tracking data and K-band range rate data of the time interval between July 2003 and August 2009 using the Celestial Mechanics Approach (Jäggi et al. 2011). The model is complete up to d/o 150 for the static field and contains secular terms of d/o 2–30.

2.2 Earth's Mean Time-Variable Gravity Field Models Containing Also Periodic Variations of Geopotential Coefficients

Table 2 contains a list of Earth's mean TVG models containing secular terms and periodic variations of geopotential coefficients. For each of these models, the time-variable part of the geopotential consisting of secular and periodic (annual and semi-annual) variations of geopotential coefficients is given for the same range of the d/o terms.

---

[3] https://ids-doris.org/documents/BC/data/POD_configuration_Jason_Envisat_GDRB_GDRC.pdf

Table 2 Earth's mean gravity field models containing secular and periodic variations of geopotential coefficients

Model name	Year	Data time span	Max. degree of the static part	Degrees of secular and sin/cos terms	References
EIGEN-GL04S-ANNUAL	2007	Feb. 2003–Feb. 2005	150	2–50	Lemoine et al. (2007)
EIGEN-6S	2011	Jan. 2003–Jun. 2010	240	2–50	Förste et al. (2011)
EIGEN-6C	2011	Jan. 2003–Jun. 2010	1420	2–50	Shako et al. (2014)
EIGEN-6C2	2013	Jan. 1985–Apr. 2011	1949	2–50	Förste et al. (2013)
EIGEN-6S2	2014	Jan. 1985–May 2013	260	2–50[a]	Rudenko et al. (2014)
EIGEN-GRGS.RL02bis.MEAN-FIELD	2012	Mar. 2003–Mar. 2011	160	1–50	CNES (2012)
EIGEN-6S2.extended.v2	2014	Jan. 1985–Dec. 2013	260	2–50[a]	Rudenko et al. (2014)
EIGEN-GRGS.RL03-v2.MEAN-FIELD.mean_slope_extrapolation	2014	Jan. 1985–Dec. 2013	300	2–80[a]	Lemoine et al. (2014)
EIGEN-6S4_v2	2016	Jan. 1985–Jul. 2014	300	2–80[a]	Förste et al. (2016)
EIGEN-GRGS.RL04.MEAN-FIELD	2018	Jan. 1985–Jun. 2016	300	2–90[a]	Lemoine et al. (2018)
GOCO05s	2015	Feb. 2003–Dec. 2013	280	2–100	Mayer-Gürr et al. (2015)
GOCO06s	2019	Apr. 2002–Aug. 2016	300	2–200	Kvas et al. (2021)
ITSG-Grace2014k	2014	Feb. 2003–Dec. 2013	200	2–100	Mayer-Gürr et al. (2015)
ITSG-Grace2014s	2014	Feb. 2003–Dec. 2013	200	2–100	Mayer-Gürr et al. (2015)
ITSG-Grace2018s	2019	Apr. 2002–Jun. 2017	200	2–200	Kvas et al. (2019)
CNES_GRGS.RL05MF_combined_GRACE_SLR_DORIS	2023	Jan. 1980–Oct. 2022	300	2–90[a]	Lemoine et al. (2023)
COST-G Deterministic Signal Model	2025	2018–2025	90	2–90	Peter et al. (2022)

[a]Time-dependent values of secular and periodic terms

2.2.1 EIGEN-GL04S-ANNUAL

EIGEN-GL04S-ANNUAL (Lemoine et al. 2007) is the first Earth's mean gravity field model of which the time-variable part contains, besides secular terms, also annual and semi-annual (sine and cosine) variations of geopotential coefficients. This model is complete up to d/o 150 and contains above mentioned time-variable coefficients for d/o 2–50. The values of the secular and periodic terms are constant for each spherical harmonic coefficient over the complete time span of modeling. The model was derived from a two-year (February 2003 to February 2005) time span of GRACE and LAGEOS-1/2 data. Its reference date is 2004.0. The secular terms were determined over only two years (2003–2005). This model was selected for the GDR-C altimetric orbit standards.[4]

2.2.2 EIGEN-6S, EIGEN-6C and EIGEN-6C2

EIGEN-6S (Förste et al. 2011) is a satellite-only model based on LAGEOS-1/-2 SLR data and GRACE GPS-SST and K-band range rate data from January 2003 to June 2009, as well as GOCE Satellite Gravity Gradiometry Txx, Tyy, and Tzz data from November 2009 to June 2010. The time-variable part of the model consists of a secular term, cosine and sine terms of annual and semi-annual variations of each spherical harmonic coefficient up to d/o 50. EIGEN-6C (Shako et al. 2014) is the first global combined TVG model that includes also GOCE data. It was computed from a combination of LAGEOS-1/-2, GRACE, and GOCE data, enhanced with the DTU10 surface gravity data. The initial release of EIGEN-6C published in 2011 was complete up to d/o 1440, while the second release of this model published in 2012 was complete up to d/o 1990. EIGEN-6C2 (Förste et al. 2013) is an update of EIGEN-6C. It is complete up to d/o 1949 and is based on the extended measurement time spans for the LAGEOS, GRACE, and GOCE data, namely

- LAGEOS SLR data from January 1985 until December 2010,
- GRACE (GPS-SST and K-band range rate) data from March 2003 until December 2010,
- GOCE (satellite gradiometry only) data from 1 November 2009 till 19 April 2011.

2.2.3 EIGEN-GRGS.RL02bis.MEAN-FIELD, EIGEN-6S2, EIGEN-6S2.extended.v2, and EIGEN-6C2

EIGEN-GRGS.RL02bis.MEAN-FIELD (CNES 2012) is based on eight years of GRACE and LAGEOS data (March 2003–March 2011). The model is complete up to d/o 160. Its time-variable part consisting of secular terms, annual and semi-annual sine and cosine variations of geopotential coefficients is given for d/o 1–50. Additionally, a correction (an offset) is introduced to take into account the permanent deformation of the gravity field associated with the Sumatra earthquake on 26 December 2004. The reference epoch of the model is 2005.0. This is the reference gravity field model for the GDR-D altimetric standards.[5]

---

[4] https://ids-doris.org/documents/BC/data/POD_configuration_Jason_Envisat_GDRB_GDRC.pdf

[5] https://ids-doris.org/documents/BC/data/POD_configuration_GDRE.pdf

EIGEN-6S2 (Rudenko et al. 2014) was derived using a longer time span of data, namely:

- LAGEOS-1/-2 SLR data from 1985 to 2010,
- GRACE normal equations were used from the GRGS release 02 GRACE processing for the time span February 2003–January 2011 and the GFZ release 05 processing for the time span October 2003–September 2012,
- the GOCE part includes, in addition to Vxx, Vyy, and Vzz, also the Vxz component.

The difference in the coefficients representation for this model, as compared to EIGEN-6S, consists in the fact that the coefficients of Eq. 1 of this model are no longer constant over the complete time span of modeling, but are time-variable. Thus, the coefficients are given with a one-year time step from 9 January 1985 until 1 January 2012 for degree 2 terms and from 1 January 2003 until 1 January 2012 for degree 3–50 terms (measurement period). Zero values of the secular terms and periodic corrections are used outside of the measurement period (the time span of input data).

EIGEN-6S2.extended.v2 (Rudenko et al. 2014) is an extended version of EIGEN-6S2 in which the TVG part was extended beyond 2012.0, until 2014.0, using the mean slopes of 2009.0–2012.0 for the slopes of 2012.0–2014.0. This model was selected and used for ITRF2014 computation.

2.2.4 EIGEN-GRGS.RL03-v2.MEAN-FIELD.mean_slope_extrapolation

This model (Lemoine et al. 2014) is complete up to d/o 260. It is based on GOCE-DIR5 for the part between degree 81 and 260. The TVG coefficients between degrees 1 and 80 are obtained from a regression on the GRGS-RL03-v2 monthly time series (2002.5–2014.5). For degree 2, this TVG part is extended to 1985–2014.5 through the use of a GRGS SLR-only (LAGEOS-1 and LAGEOS-2) solution between 1985 and 2003. Outside of the measurements period (1985–2014.5 for degree 2, 2003–2014.5 for degrees 3–80), the gravity field is extrapolated by the average slope of the signal over the period 2003.0–2014.0.

The modeling of the TVG part includes, as for EIGEN-6S2, two annual and two semi-annual coefficients for each year, in addition to one bias and one secular term for each year. The bias and secular term are, in general, coherent so that the result is a piecewise linear function, except in the case of earthquakes. Three major earthquakes were introduced in the modeling: Sumatra on 26 December 2004, Concepcion on 27 February 2010 and Tōhoku on 11 March 2011. This model was selected for the GDR-E orbit standards.[6]

2.2.5 EIGEN-6S4_v2 and EIGEN-GRGS.RL04.MEAN-FIELD

EIGEN-6S4 (version 2) (Förste et al. 2016) is a satellite-only global gravity field model derived by the combination of LAGEOS, GRACE, and GOCE data. The model is complete up to d/o 300. Its time-variable part consisting of secular terms as well as annual and semi-annual variations per year includes d/o 2–80. The model was derived using LAGEOS-1/2 SLR observations from 1985 to 2003, GRACE-LAGEOS monthly gravity fields from August 2002 to July 2014, as well as GOCE data processed via the direct numerical

---

[6] https://ids-doris.org/documents/BC/data/POD_configuration_GDRE.pdf

approach. The model includes an improved modeling of the TVG part, in particular, for $C_{2,0}$.

EIGEN-GRGS.RL04.MEAN-FIELD (Lemoine et al. 2018) is complete up to d/o 300. It is based on GOCE-DIR5 for the part between degree 91 and 300. The modeling of the TVG part of this model is identical to the one of the EIGEN-GRGS.RL03-v2.MEAN-FIELD.mean_slope_extrapolation model with a difference that the maximum d/o of the TVG part was increased from 80 to 90. The TVG coefficients between degrees 1 and 90 were obtained from a regression on the GRGS-RL04-v1 monthly time series of solutions (September 2002–June 2016). For degrees 1 and 2, this TVG part is extended to January 1993–February 2019 through the use of a GRGS SLR-only solution based on the data of five SLR satellites (LAGEOS-1, LAGEOS-2, Starlette, Stella, and Ajisai). As for the previous CNES model, three major earthquakes were introduced. Outside of the measurements period (January 1993–February 2019 for degrees 1 and 2, September 2002–June 2016 for degrees 3 to 90), the gravity field is extrapolated using a mean slope computed using only the last two years (2014–2016) of the data span. This model was selected for POE-F orbit standards.[7]

2.2.6 ITSG-GRACE Models

ITSG-GRACE is a series of Earth's gravity field solutions computed at the Institute of Geodesy of the Graz University of Technology. Published models include ITSG-Grace2014s and ITSG-Grace2014k (Mayer-Gürr et al. 2015), and ITSG-GRACE2018S (Kvas et al. 2019). The later model was derived using GRACE data for the period between April 2002 and August 2016. The model is complete up to d/o 200. The TVG part of the model is provided for degrees 2–200. However, on the contrary to the TVG models described just before, no semi-annual variations (but only annual variations) are provided for the spherical harmonic coefficients of this model. Moreover, the secular term and annual variations are constant for each spherical harmonic coefficient of this model over the complete time span.

2.2.7 GOCO Models

GOCO (Gravity Observation Combination) models were derived by the GOCO consortium consisting of five institutions (Fecher et al. 2017). The main objective of the consortium is to compute high-accuracy and high-resolution global gravity field models from complementary gravity data sources: satellite gravity missions CHAMP, GRACE, and GOCE, SLR data (satellite-only models of the GOCO-S series), and additionally terrestrial gravity field and satellite altimetry data (combined GOCO-C models). The combination is done by superposition of full normal equations and applying optimized relative weighting strategies. Among satellite-only models, GOCO05S (Mayer-Gürr et al. 2015) and GOCO06S (Kvas et al. 2021) were published. GOCO06S is complete up to d/o 300. The model was derived using the following data:

- GOCE TIM6 gradiometer observations (data of the complete mission period),
- GRACE data from April 2002 until August 2016 (ITSG-GRACE2018s model),

---

[7] https://ids-doris.org/documents/BC/data/POD_configuration_POEF.pdf
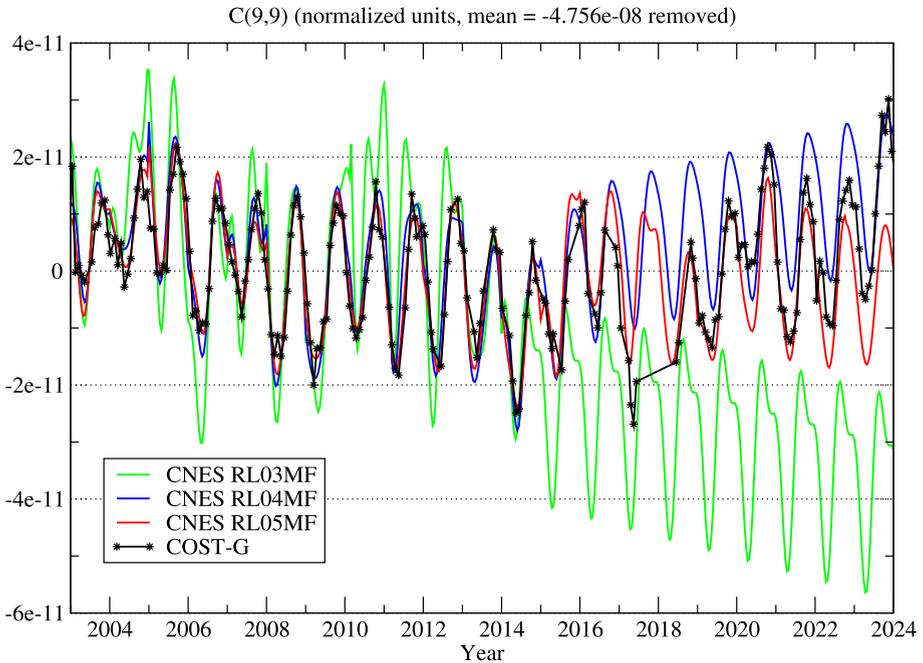
Fig. 1 $C_{9,9}$ coefficient time evolution for three CNES mean fields and for the COST-G combined solution

- kinematic orbits of Swarm-A/-B/-C, TerraSAR-X, TanDEM-X, CHAMP, GRACE-A/-B, and GOCE (TIM6 SST),
- SLR observations to LAGEOS-1, LAGEOS-2, Starlette, Stella, Ajisai, LARES, Larets, Etalon-1, Etalon-2, and BLITS from April 2002 until August 2016.

As for ITSG-GRACE2018S, the TVG part of the model is provided for degrees 2–200 and only annual (but no semi-annual) variations are available for the spherical harmonic coefficients of this model, and the secular term and annual variations are constant for each spherical harmonic coefficient over the complete time span.

2.2.8 COST-G Deterministic Signal Model

This model is derived by the International Combination Service for Time-variable Gravity Fields (COST-G) using GRACE-FO measurements (Peter et al. 2022). $C_{2,0}$ is replaced by the GRACE-FO+SLR combined solution. The model is complete up to d/o 90, secular and periodic (annual and semi-annual) terms are provided for d/o 2–90. The values of the secular and periodic terms are constant over the complete time span of the model from 1 January 2018 until now for each gravity field coefficient.

2.2.9 CNES_GRGS.RL05MF_combined_GRACE_SLR_DORIS

This model is based on 30 years (1993–2022) of SLR data, 10 years (1993–2002) of DORIS data, 21 years (2002–2022) of GRACE/GRACE-FO data and 3.5 years (November
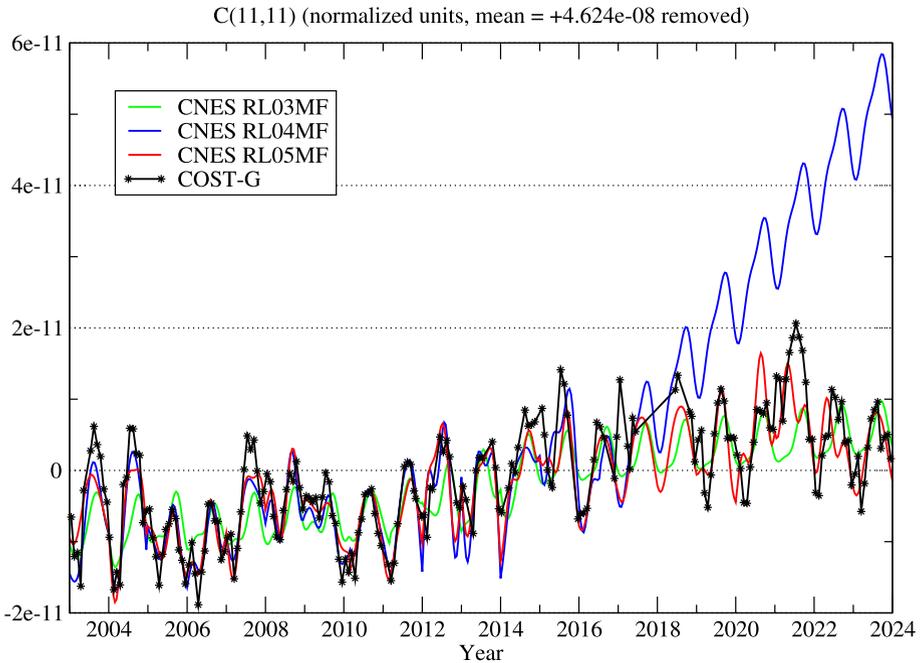
Fig. 2 $C_{11,11}$ coefficient time evolution for three CNES mean fields and for the COST-G combined solution

2009–October 2013) of GOCE data and is complete up to d/o 300. More specifically, the following data were used to derive this model (Lemoine et al. 2023):

- DORIS+SLR mascons from January 1993 to March 2002. SLR data for LAGEOS-1, LAGEOS-2, Starlette, Stella, Ajisai, and Lares satellites starting in 1980, DORIS data for all DORIS-carrying satellites, from TOPEX/Poseidon to HY2A and SARAL. The mascons solution was converted to spherical harmonics between degree 1 and 40,
- GRACE+SLR RL05 monthly gravity field time series between April 2002 and October 2022,
- GOCE-DIR5 for the static part between degree 91 and 300.

The TVG part of the model is provided for degrees 1–90. The coefficients are given with a one-year time step from 17 January 1993 until 16 October 2022 for degrees 1–90. The retrograde extrapolation of the secular term coefficients (pre-1993) was obtained from a regression on the DORIS+SLR mascons. The prograde post-2022 extrapolation of the coefficients of secular terms was obtained from a regression over the GRACE era (2002–2022). As for the two previous GRGS models, three major earthquakes were introduced.

Figure 1 illustrates exemplarily the improvements from CNES RL03MF to RL05MF and the difficulty of extrapolating the mean fields. COST-G time series of d/o 9 is used here as a reference for the evaluation of the mean fields. RL03MF was over-estimating, for this coefficient, the annual cycle. Its extrapolation based on the average slope between 2003 and 2014 was not successful in representing the real evolution of the $C_{9,9}$ coefficient. Both RL04MF and RL05MF have a better representation of the actual time evolution of this coefficient over their respective GRACE/GRACE-FO data inclusion periods,

2002.5–2014.5 and 2002.5–2022.5, respectively. The extrapolation of RL04MF based on the slope of the last two years before the end of the data is more successful than the one of RL03MF for that coefficient, but can be very wrong for other coefficients as illustrated by Fig. 2 which plots coefficient $C_{11,11}$. We have selected these spherical harmonic coefficients and this time span, since one can clearly see the differences in the coefficient time series from various models at the time spans beyond those ones used to derive respective gravity field models. It is also clear from these figures that the mean fields, with only one bias, one slope, annual and semi-annual periodic coefficients per year, cannot represent the TVG as accurately as the monthly solutions. This consideration strengthens the need to have regular updates of the mean fields, with an extrapolation period not exceeding one year. Therefore, an update of this model CNES_GRGS.RL05MF_2024_08.shc is available since January 2025 at.[8] Compared to the original model, it incorporates 22 additional monthly GRACE-FO solutions from CNES RL05 (November 2022 to August 2024). These GRACE-FO monthly solutions include SLR data from six satellites: LAGEOS-1, LAGEOS-2, Starlette, Stella, Ajisai, and Lares. This model was selected for the POE-G orbit standards.[9]

3 Precise Orbit Determination

To see the impact of various Earth's mean TVG models on orbits of altimetry satellites and altimetry results, we selected nine models given in Table 3. The selected models represent the latest versions of the Earth's mean TVG models of each generation (release) published in 2011–2023, as far as CNES/GRGS models concerns, and the latest releases of GOCO and ITSG-GRACE series of models. To show the impact of earlier models on orbit quality, we have added three more models, namely, the GRIM5-C1 model derived in 2000 without using any CHAMP and GRACE data, the EIGEN-GL04S1 model developed in 2006 using 30 months of GRACE data covering the period from February 2003 until July 2005 and 24 months (February 2003 to February 2005) of LAGEOS SLR data used for accurate estimation of $C_{2,0}$ and EIGEN-6S developed in 2011. We have not included in our tests the COST-G deterministic signal model, since this model is derived using data starting from June 2018 and, therefore, it has to be extrapolated for the time intervals before this time instant resulting in degraded orbit quality for the time spans before June 2018.

We have performed POD for four altimetry satellites at the following time spans: TOPEX/Poseidon (27 September 1992 – 9 October 2005), Jason-1 (13 January 2002 – 30 June 2013), Jason-2 (20 July 2008 – 2 October 2019), and Jason-3 (17 February 2016 – 28 June 2023). We use the DGFI-TUM Orbit and Geodetic parameter estimation Software (DOGS, Gerstl 1997; Bloßfeld 2015) for POD. Orbits are computed generally at 3.5-day long arcs. A bit shorter or longer arcs are used in the vicinity of orbit maneuvers. We use SLR observations available from the International Laser Ranging Service (ILRS, Pearlman et al. 2019) in POD, since SLR observations are more sensitive to the changes of the Earth's gravity field models than GPS or DORIS observations during the analysis of which many parameters are estimated that can absorb the differences caused by a model replacement. The main models used in the POD of this study are provided in Tables 5, 6, 7, 8 and 9. We use SLRF2020 (Pavlis and Luceri 2022) being an extension of ITRF2020

---

[8] https://grace.obs-mip.fr/variable-models-grace-lageos/mean-fields/release-05/

[9] https://ids-doris.org/documents/BC/data/POD_configuration_POEG.pdf

Table 3 Earth's mean TVG models used for the POD tests

Model name	Model name abbreviation	Data time span	Max. degree of the static part	Max. degree of the time-variable part	References
GRIM5-C1	GRIM5-C1	1971–1998, 2000	120	2–4	Gruber et al. (2000)
EIGEN-GL04S1	EIGEN-GL04S1	2003–2005	150	2–4	Förste et al. (2008b)
EIGEN-6S	EIGEN-6S	1985–2009	240	50	Förste et al. (2011)
EIGEN-6S2.extended.v2	EIGEN-6S2ext2	1985–2014	260	50	Rudenko et al. (2014)
EIGEN-GRGS.RL03-v2.MEAN-FIELD.mean_slope_extrapolation	CNES RL03MF	1985–2014	300	80	Lemoine et al. (2014)
ITSG-GRACE2018S	ITSG-GRACE2018S	2002–2017	200	200	Kvas et al. (2019)
GOCO06S	GOCO06S	2002–2017	300	200	Kvas et al. (2021)
EIGEN-GRGS.RL04.MEAN-FIELD	CNES RL04MF	1985–2016.5	300	90	Lemoine et al. (2018)
CNES_GRGS.RL05MF_combined_GRACE_SLR_DORIS	CNES RL05MF	1980–2022	300	90	Lemoine et al. (2023)

(Altamimi et al. 2023) for SLR stations that includes also historical and very recently installed SLR stations that are missing in ITRF2020. We apply LAGEOS-1 SLR long-term mean range biases from the ILRS Data Handling File (DHF) for SLRF2020 (Data Handling File 2024) for SLR observations of all altimetry satellites, as it is recommended in this DHF. An advantage of applying these long-term mean range biases for POD of altimetry satellites has been shown by Rudenko et al. (2025). SLR observations having time biases ≥ 10 μs were excluded during SLR observation screening. A list of parameters estimated at each orbital arc together with the frequency of their estimation and their a priori standard deviation (sigma) is given in Table 4.

4 Impact on Orbital Parameters

First, we analyze the POD results over the complete time span from September 1992 to June 2023 of all four altimetry satellites of this study. Analyzing the RMS values of SLR observation residuals shows (Fig. 3a) that the CNES RL04MF and CNES RL05MF models provide the smallest average value of this parameter (1.91 cm), while the GRIM5-C1 model provides the largest (2.37 cm) average value of this parameter over the complete time span. A more detailed analysis shows that CNES RL05MF performs better than CNES RL04MF at the time span 2016–2023. The GOCO06S and ITSG-GRACE2018S models show trends in the cross-track empirical acceleration in 1992–2005 (Fig. 3b), since the secular terms and annual variations of the gravity field coefficients determined over 2002–2016 for these models have to be used outside of this time span, and since they are constant for each coefficient over the complete time span. This shows importance of modeling the time-variable part of the Earth's gravity field at the complete time span at which satellites orbits are to be computed, not just at the GRACE time span. GRIM5-C1 and EIGEN-GL04S1 provide the largest scatter of empirical acceleration (Fig. 3b) that absorbs mismodeling coming from these gravity field models. The largest absolute mean values of empirical accelerations are obtained for ITSG-GRACE2018S and GOCO06S models, showing TVG mismodeling that has been absorbed by larger absolute values of empirical accelerations. On the contrary, Figs. 3 and 4b show that CNES RL04MF and RL05MF models provide smallest standard deviations of empirical acceleration indicating that it is least scattered. The average values

Table 4 A list of estimated parameters

| Parameter	Frequency	A priori sigma
Keplerian elements	Once per arc	Unconstrained
Solar radiation pressure scale factor	Once per arc	0.1 [–]
Earth's albedo and infrared radiation scale factor	Once per arc	0.1 [–]
Atmospheric drag scale factor	Every 12 h	0.1 [–]
Empirical acceleration (sine and cosine terms of the cross-track and along-track components)	Once per arc	$1.34 \cdot 10^{-9}$ [m/s^2]
Empirical acceleration (coefficient of a continuous piecewise linear function of the cross-track and along-track components)	Every 12 h	$1.34 \cdot 10^{-9}$ [m/s^2]
SLR range bias of selected stations	Once per arc	0.1 [m]

(a)

(b)
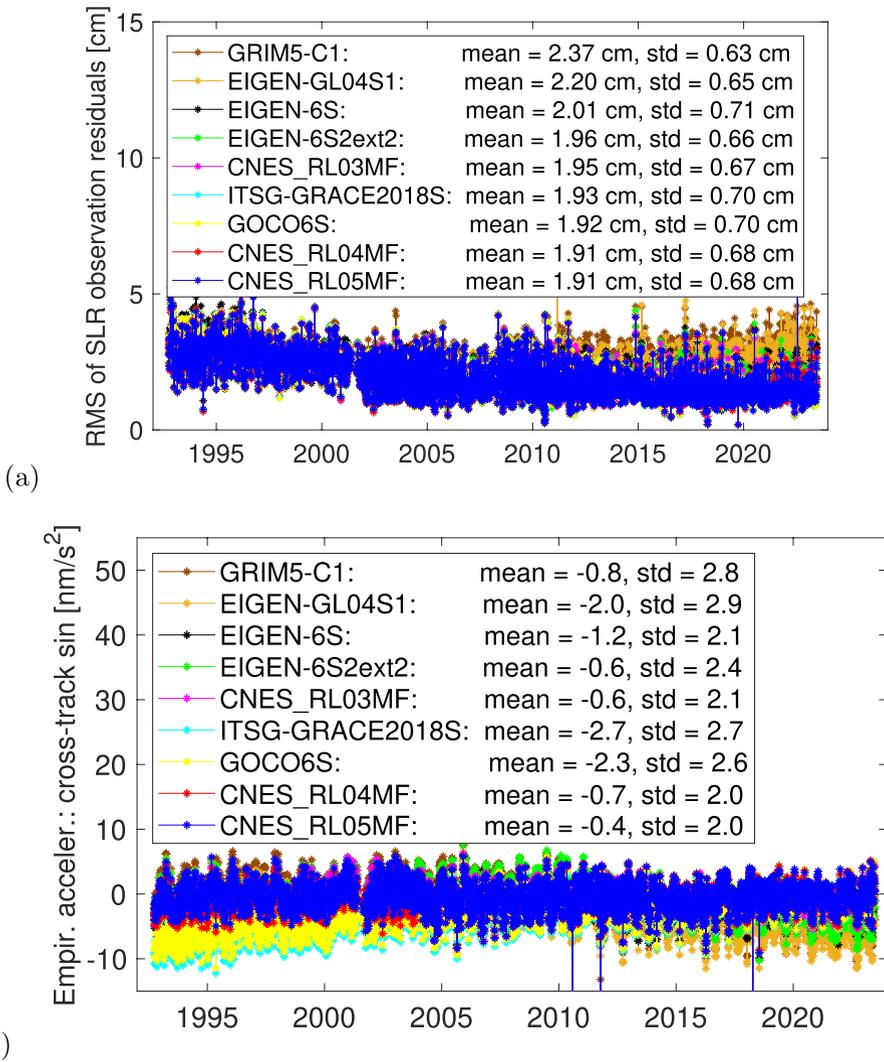
Fig. 3 Time series of the (**a**) arc-wise RMS values of SLR observation residuals and (**b**) sine term of the cross-track empirical acceleration over the time span of all four altimetry satellites obtained using various gravity field models

of the mean of SLR observation residuals are of 0.06–0.07 cm for most models, except EIGEN-6S that provides a larger value of 0.09 cm for this parameter.

Jason-3 is of particular interest for this study, since the time span of its orbit (February 2016–June 2023) covers the periods of the last months of GRACE data, a gap between GRACE and GRACE-FO and a period of GRACE-FO data used to derive the CNES RL05MF model. Therefore, we analyze the results for this satellite in more details. An impact of the gravity field models on the mean and standard deviations of the following orbital parameters of Jason-3 is shown in Fig. 4: RMS and mean values of SLR observation residuals, scale factors of the solar radiation pressure (SRP), Earth's

(a)

(b)
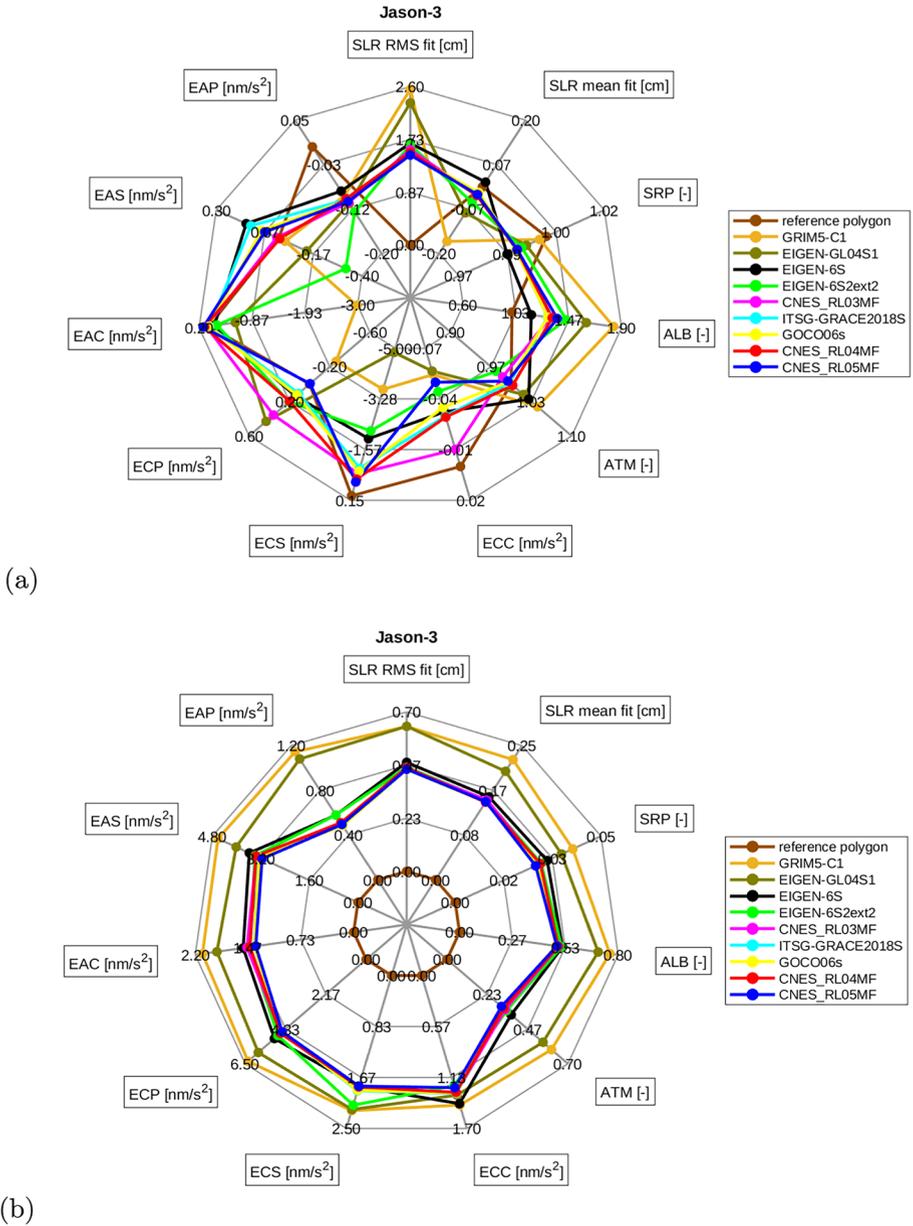
Fig. 4 Mean (**a**) and standard deviations (**b**) of orbital parameters of Jason-3 obtained using various gravity field models

albedo and infrared radiation (ALB), atmospheric drag (ATM), sine (S), cosine (C), and piecewise linear (P) terms of the along-track (EA) and cross-track (EC) empirical accelerations. These so-called spider plots show how close the average values of the

respective orbit parameters are to the nominal values forming a reference polygon. The values of the reference polygon are equal to zero for the residuals and accelerations and to 1 for the scale factors, since this would mean perfect values of these parameters. The closer the average values are to the reference polygon, the better is the performance of the respective model. The smallest average value of the RMS of SLR observation residuals (1.48 cm) is obtained for this satellite using CNES RL05MF indicating that this model performs best among the nine models tested for this satellite, whereas the largest average value (2.56 cm) is obtained for GRIM5-C1 indicating its worst performance. The smallest absolute mean values of SLR observation residuals (0.01–0.05 cm) are obtained for the seven most recent models tested, while GRIM5-C1 and EIGEN-GL04S1 provide the largest absolute values (0.08–0.16 cm) of this parameter. A replacement of the Earth's gravity field model does not impact the scale factor of the solar radiation pressure significantly: the values are within 0.987–0.998 for various models. The values of the scale factor of the atmospheric drag closest to 1 (0.99–1.00) are obtained for the latest four gravity field models, i.e., ITSG-GRACE2018S, GOCO06S, CNES RL04MF, and CNES RL05MF, whereas five older models, i.e., GRIM5-C1, EIGEN-GL04S1, EIGEN-6S, EIGEN-6S2ext2, and CNES RL03MF, provide average values of 0.98–1.04 that differ more significantly from the nominal value. This indicates that some mismodeling of five older Earth's gravity field models is absorbed by the scale factor for atmospheric drag acting in the along-track direction. Empirical accelerations absorb unmodeled or mismodeled effects affecting the satellite orbit, including those coming from TVG. Standard deviation characterizes, how the time series is scattered. Mean value specifies a bias. Absolute values of empirical accelerations in the cross-track and along-track directions are about 3–8 times larger for GRIM5-C1, EIGEN-6S, and EIGEN-6S2ext2, than for other models. Figure 4b clearly shows that the standard deviations of most orbital parameters obtained using the CNES RL05MF model are closer to the nominal values being 0, while those obtained using GRIM5-C1, EIGEN-GL04S1, and EIGEN-6S are the largest for most orbital parameters indicating their larger scatter around the average values. We conclude from this analysis that the CNES RL05MF model provides the best performance for Jason-3 among the nine models used in these tests.

To quantify the impact of the Earth's gravity field models on orbit differences in the radial direction, we provide the RMS and mean values of radial orbit differences of Jason-3 orbits derived using CNES RL05MF (reference solution, since this model shows the best performance among the models tested) and other gravity field models of Table 3 in Fig. 5. GRIM5-C1 provides significant orbit differences in the radial direction w.r.t. CNES RL05MF with the RMS values of 1.88 cm. For the recently developed models, the RMS values of orbit differences in the radial direction fit within 0.7–0.8 cm with smallest values provided by CNES RL04MF and GOCO06S. A trend in the RMS values of radial orbit differences visible for EIGEN-6S and CNES RL04MF, as compared to CNES RL05MF, as well as increasing (with time) scatter of the mean values of radial orbit differences for all models shown in Fig. 5b are due to the extrapolation errors of these models, derived using the data of the time spans by 2017, at the Jason-3 time span of 2016–2023.5. GRIM5-C1 provides significantly larger (0.34 cm) absolute mean values of radial orbit differences w.r.t. CNES RL05MF than other models.
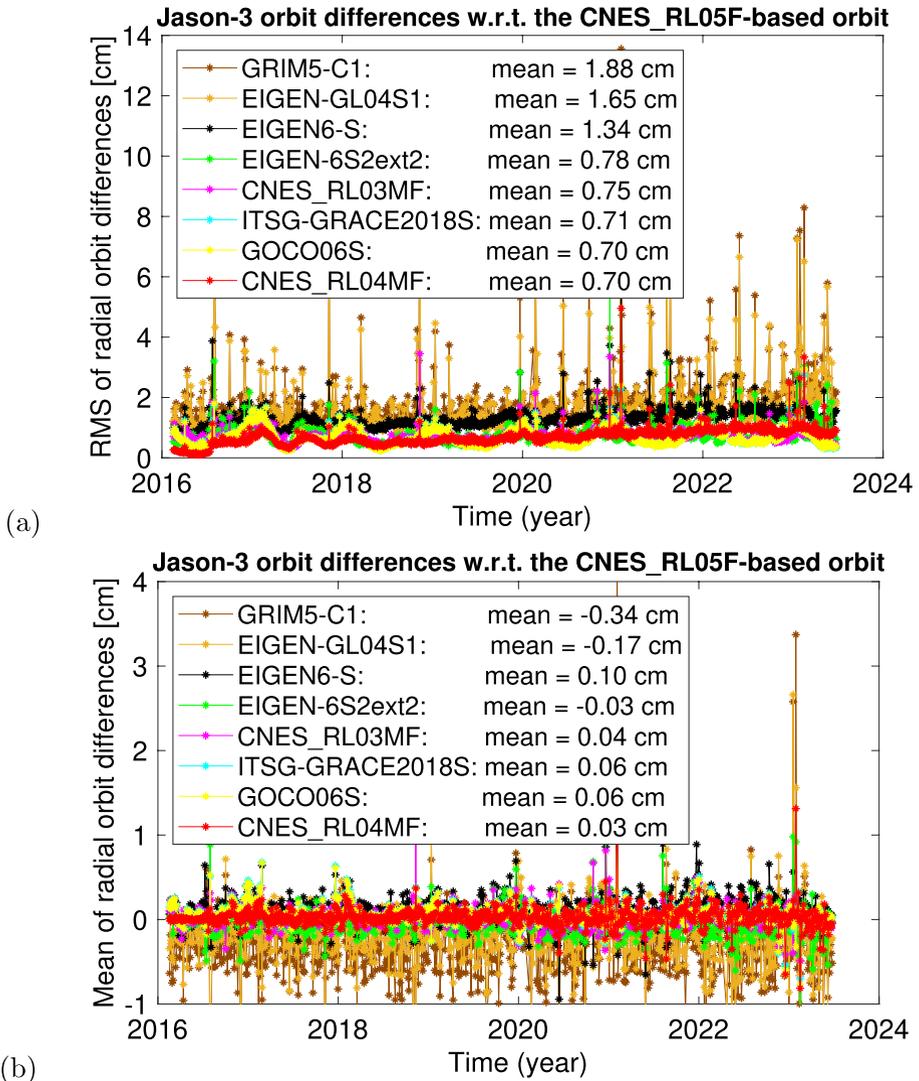
Fig. 5 RMS (**a**) and mean (**b**) values of radial orbit differences of Jason-3 orbits derived using CNES RL05MF (reference) and other gravity field models of Table 3

5 Altimetry Crossover Results

In order to investigate the impact of different gravity field models used for orbit computations on satellite altimetry results and sea level determination, sea surface height (SSH) crossover differences are analyzed. Based on the results of POD tests (Sect. 3), we choose only the seven mean gravity field models from Table 3 developed since 2011. For this purpose, in a first step, the seven different orbit solutions for Jason-2 and Jason-3 are used to compute SSH and to build single-satellite crossover differences (SXO) between ascending

and descending passes with a time limit of two days. For each 10-day cycle of the missions, the means and standard deviations of these SXO are analyzed.

Figure 6 shows the average mean values and standard deviations of the SXO for both satellites and all available orbit solutions. It should be noted, that the absolute numbers include not only the effects due to orbit uncertainties but also all other components of SSH, such as measurement uncertainties and errors in geophysical corrections. Therefore, the Jason-2 and Jason-3 numbers are not directly comparable, neither with each other nor with results from other groups that may use different time limits to define the crossover points. Only the differences between the solutions based on different gravity fields should be analyzed. The top plot shows the mean SXO. For Jason-2, their absolute values are less than 1.5 mm for all orbit solutions, and the differences between the solutions are not significant. For Jason-3, however, the absolute values are much larger and all exceed 3 mm, except for the latest solution CNES RL05MF. In particular, the value of about -8 mm for EIGEN-6S indicates systematic errors in this gravity field for the Jason-3 time period.

Looking at the standard deviations, it can be seen that for both missions, the newer models generally perform better than the older ones. However, the differences are quite small: only 0.5 mm for Jason-2. For Jason-3, the differences are about twice as large: up to 1.2 mm. The older EIGEN models are clearly worse than ITSG-GRACE2018s, GOCO06S, and CNES RL05MF.

The data also allow an analysis of the temporal evolution of SXO. Computing the differences in SXO statistics between the EIGEN-6S and CNES RL05MF results (Fig. 7, black points), a temporal drift in both the means and the standard deviations can be clearly seen, indicating a decreasing performance of EIGEN-6S (developed using the data of 1985–2009) over the years of 2016–2022, i.e., at the extrapolation time interval. The differences in the SXO statistics between the CNES RL04MF and CNES RL05MF results (Fig. 7, red points) also indicate a trend caused by the computation of the secular terms of the CNES RL04MF geopotential model just over two years (2014–2016) and the extrapolation over the Jason-3 time span (2016–2022). However, this trend is smaller than that one obtained for the differences between EIGEN-6S and CNES RL05MF, since the measurement period of CNES RL04MF is closer to the Jason-3 time span than that of EIGEN-6S.
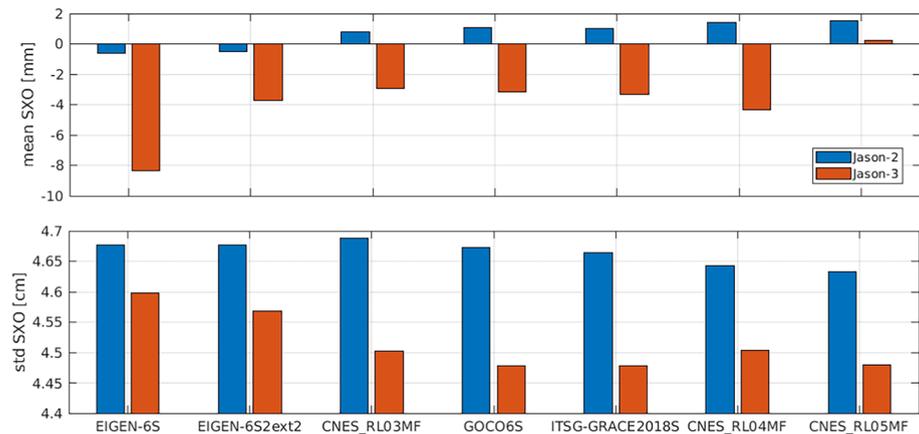

Fig. 6 Single-satellite crossover (SXO) statistics for Jason-2 and Jason-3
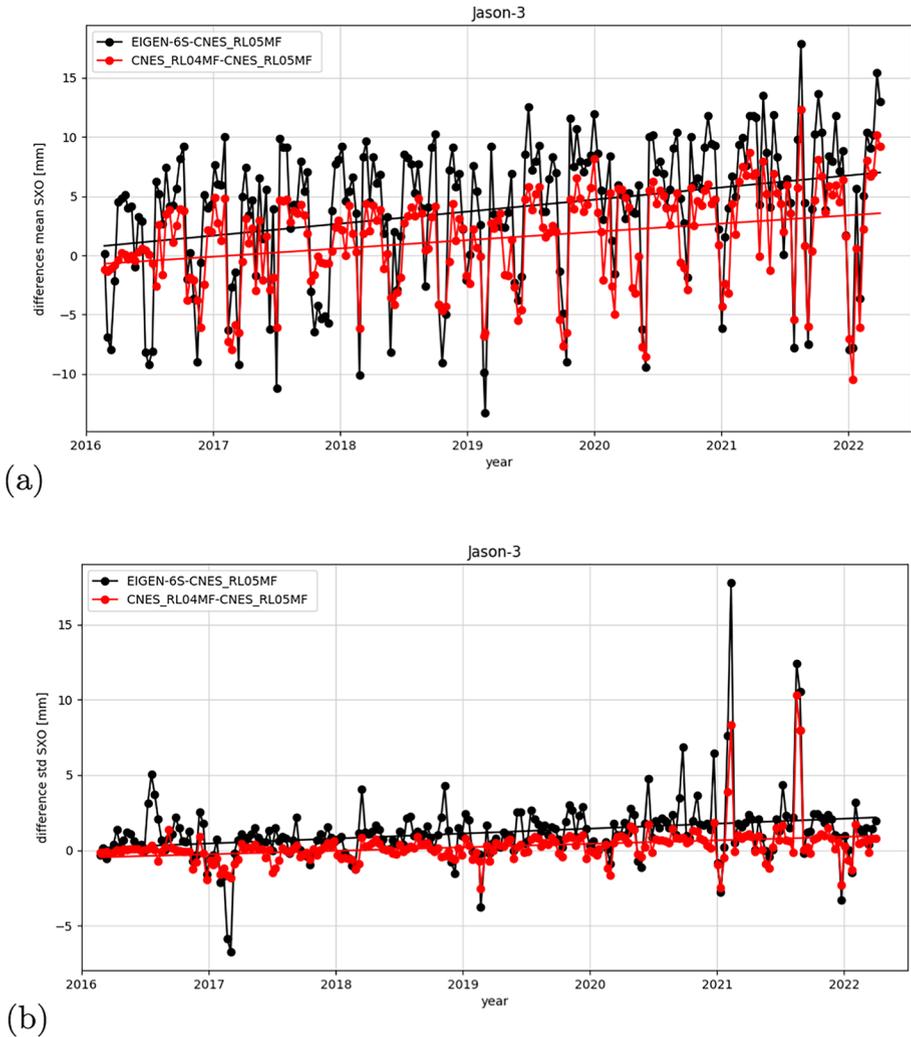
Fig. 7 Differences between means (**a**) and standard deviations (**b**) of single-satellite crossover differences between solutions based on EIGEN-6S and CNES RL04MF w.r.t. those based on the CNES RL05MF gravity field model for Jason-3

If, in addition to the single-satellite crossover differences, one also analyses differences to other missions, a so-called multi-mission crossover analysis (MMXO) can be used to calculate time series of radial errors for all missions and derive geographically correlated mean errors (GCE). The theory for this was already developed in the early years of satellite altimetry (e.g., Rosborough (1986), Klokočník and Wagner (1999), Klokočník et al. (2004)) and since then dual-satellite crossover differences have been used for many different missions and applications (e.g., Jolly and Moore (1995), Labroue et al. (2012), Prandi et al. (2015)). The MMXO as it is used in this study was described in detail in Bosch et al.
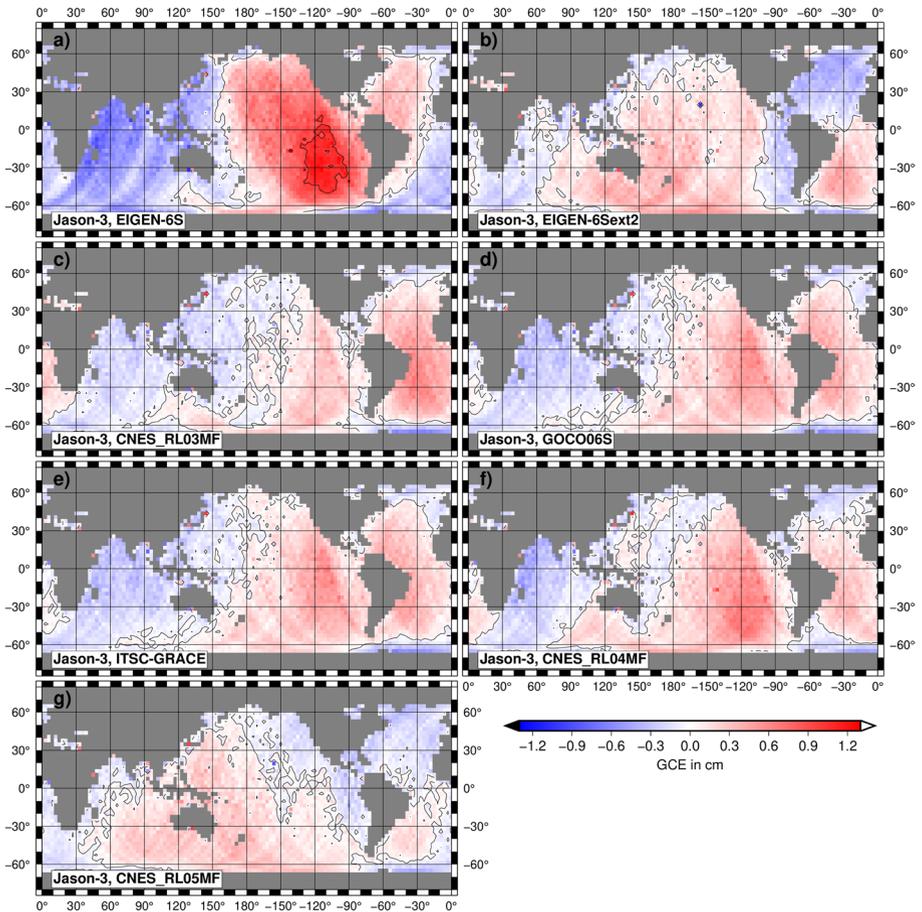
Fig. 8 Geographically correlated mean errors (GCE) of Jason-3 based on different orbit solutions computed with the seven gravity field models used in the tests. The name of the gravity field model is given within each subplot (**a**–**g**)
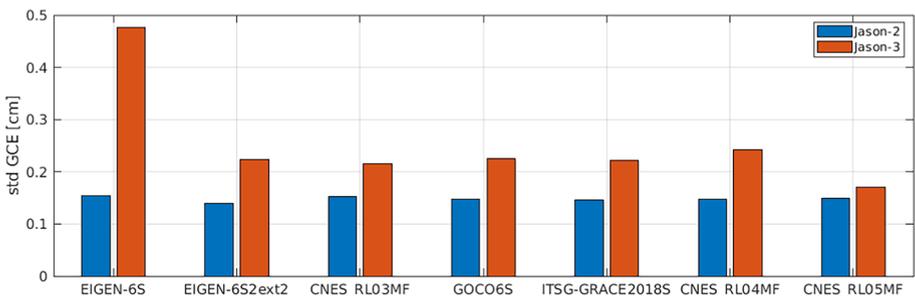

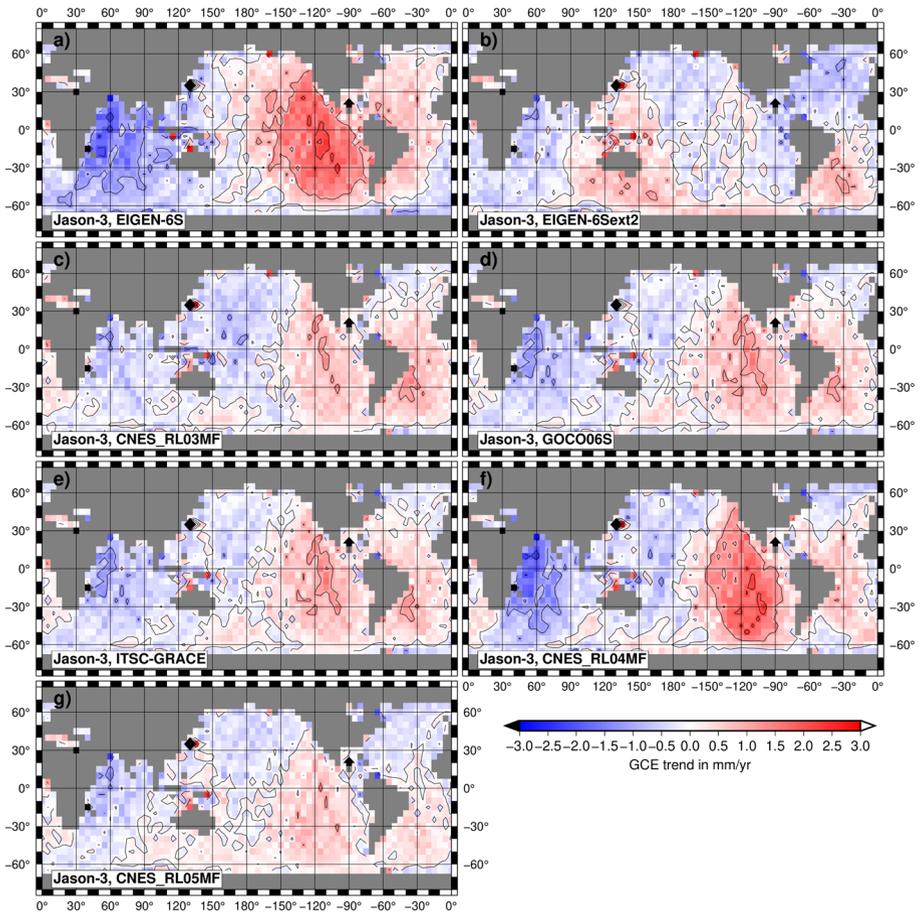**Fig. 9** Standard deviations of geographically correlated mean errors (GCE) for Jason-2 and Jason-3

Fig. 10 Trends in geographically correlated mean errors (GCE) of Jason-3 orbits computed using the gravity field models of these tests

(2014) and has already been used for evaluation of different orbits and input models, e.g., in Rudenko et al. (2014, 2018).

In this study, the Envisat, SARAL, and Sentinel-3 (A/B) missions were used in addition to the Jason satellites, depending on the time period. The data from these additional missions are identical for all runs with the different orbits for Jason-2 and Jason-3. Care was also taken to ensure that the corrections applied were selected as uniformly as possible for all missions. Nevertheless, only the differences between the solutions should be interpreted and not the absolute values, which, in addition to possible orbit effects, can contain effects due to other influences that may also be different for Jason-2 and Jason-3.

Figure 8 shows the GCE for the seven different orbit solutions for Jason-3. One can see clear differences between the solutions. In particular, the EIGEN-6S solution shows values of up to 1.5 cm with a clear east–west pattern. In contrast, the GCE of CNES RL03MF, CNES RL04MF, GOCO06S, and ITSG-GRACE2018S are significantly smaller and relatively similar. The smallest GCE are obtained for the CNES RL05MF solution. Figure 9 shows the standard deviations of these values. Larger standard deviations of

GCE for Jason-3 for all TVG models, except CNES RL05MF, are due to the extrapolation errors of these models derived using data before 2009–2017 at the time interval of Jason-3 (2016–2022). The standard deviations of GCE for Jason-2 do not show so much dependence on the TVG model, since the time span of this mission (2008–2019) is mainly within the time interval that was used to determine the TVG models or partly just shortly after that, when the extrapolation errors are still small. The Jason-2 GCE are therefore not shown here.

Since the SXO of the Jason-3 solutions show some temporal variations, it can be assumed that the GCE will also not be constant over the entire mission duration, and Fig. 8 only shows the mean values. To investigate this, the GCE were calculated for periods of six cycles each (60 days, approximately two months). A larger grid width (5° instead of 3°) was chosen in order to obtain enough observations for each location. A linear trend was then calculated for each grid point. The results for Jason-3 are shown in Fig. 10.

The computed GCE trends yield up to about 3 mm/year for EIGEN-6S and CNES RL04MF and remain below 1 mm/year for the other solutions, with the smallest values for the CNES RL05MF gravity field. The high GCE trend value of CNES RL04MF for Jason-3 can probably be explained by a short (just two-year long) time interval (2014–2016) on which the extrapolated trend was computed for this gravity field model. The same can be seen when analyzing the different components of the center-of-origin shifts. These are derived for the estimated radial errors as explained in detail in Bosch et al. (2014). The trend is clearly visible in the y-component of the EIGEN-6S results, but also for CNES RL04MF (see Fig. 11).

6 Conclusions

We have performed a review of the Earth's mean TVG models developed in 2000–2023 and available for POD of Earth orbiting satellites. The TVG part of the models developed before the GRACE mission and during its first years, i.e.,
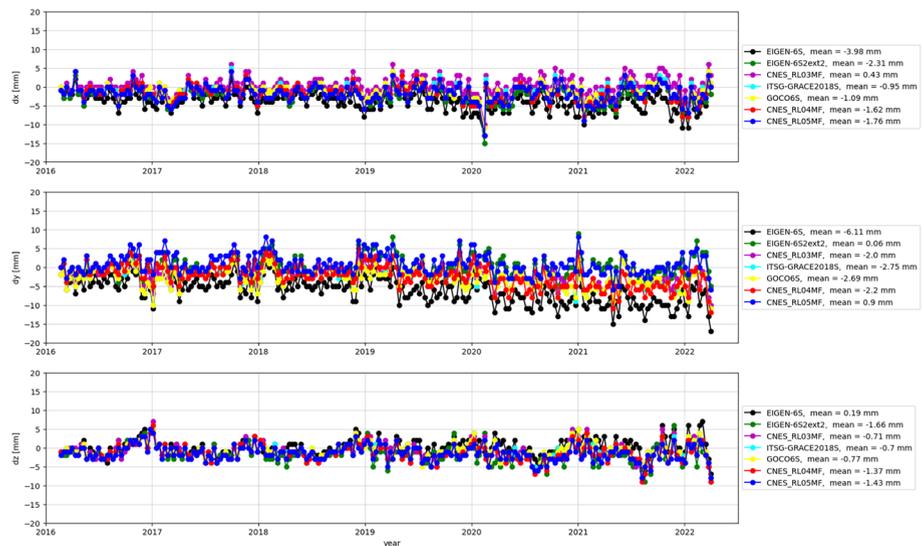

Fig. 11 The realizations of the origin (shifts in dx, dy, dz) computed for Jason-3 orbits derived using various gravity field models

in 2000–2011, consists mainly of secular terms of degree 2–4 zonal coefficients. EIGEN-GL04S-ANNUAL published in 2007 is the first Earth's mean TVG model that contains, besides secular terms, also periodic (annual and semi-annual) variations of geopotential coefficients (up to d/o 50). The amplitudes of sine and cosine variations of gravity coefficients of this model were constant over the complete time span of analyzed (GRACE) data. Analysis of the Earth's TVG using GRACE, GRACE-FO, spherical geodetic, and some non-spherical satellites using SLR and DORIS measurements allowed to model the Earth's TVG more precisely, so that the amplitudes of sine and cosine terms of annual and semi-annual variations in the latest Earth's mean TVG models, such as CNES RL05MF, are no longer constant, but change with time. The time-variable part of the latest models is provided for d/o 2–90, for some of them up to 200.

To quantify the impact of the changes in modeling of Earth's TVG in the recent TVG models on the orbits of altimetry satellites and altimetry results, we have performed POD of four altimetry satellites TOPEX/Poseidon (1992–2005), Jason-1 (2002–2013), Jason-2 (2008–2019), and Jason-3 (2016–2023) at the time spans given using nine selected gravity field models. These include the CNES/GRGS mean gravity field models of releases 2 to 5, ITSG-GRACE2018S and GOCO06S, as well as the older (GRIM5-C1, EIGEN-GL04S1, and EIGEN-6S) models. We have assessed the impact of these models on different orbit parameters, such as scale factors of the solar radiation pressure, Earth's albedo and infrared radiation, and atmospheric drag, coefficients of a sine, a cosine, and a continuous piecewise linear terms of the along-track and cross-track empirical accelerations, as well as the RMS and mean values of SLR observation residuals and orbit differences. Furthermore, the impact of the models developed in 2011–2023 on altimetry (single- and multi-satellite) sea surface height crossover differences, radial errors, geographically correlated mean errors and their trends is investigated.

Among the models tested, the CNES RL05MF model performs best, in particular for the Jason-3 time span (2016–2023), since the time-variable terms of this model were determined over the longest time span (1980–2022) among the models used in this study and covering the major part of Jason-3 time span. Additionally, GRACE, GRACE-FO, SLR observations to six spherical satellites and DORIS observations to all DORIS-carrying satellites were used for this model contributing to the improvement of its quality. The models developed without using any CHAMP, GRACE, GRACE-FO, and GOCE data show degraded orbit quality compared to the recently developed models based on these data and modeling secular, annual and semi-annual changes of gravity field coefficients. The weakest performance among the models tested is obtained for the GRIM5-C1 gravity field model, derived using the data only until 2000. Extrapolation of the TVG for this model at the time span of Jason-3 (2016–2023) causes degraded performance of all orbit parameters and altimetry analysis results.

Among the models developed in 2011–2023, the EIGEN-6S model provides notable geographically correlated errors (up to 15 mm) and about 8 mm mean single-satellite crossover differences for Jason-3 due to extrapolation errors of time-variable terms of this model, that were determined over a short time span (2003–2009). EIGEN-6S provides the largest (4.8 mm) and CNES RL05MF provides the smallest (1.8 mm) standard deviations of geographically correlated mean errors for Jason-3 among the models tested. Newer gravity field models, such as ITSG-GRACE2018s, GOCO06S, and CNES RL05MF, provide smaller standard deviations of crossover differences than the other models tested. EIGEN-6S and CNES RL04MF provide the largest (up to 3 mm/year) trends of geographically correlated errors for Jason-3. These trends are, most probably, caused by the extrapolation errors of the TVG secular terms determined either long in the past in case of EIGEN-6S or

at a short time span in case of CNES RL04MF. The GCE trend is below 1 mm/year for all other models and the smallest trend is obtained for CNES RL05MF.

The GOCO06S and ITSG/GRACE2018S models show trends in the cross-track empirical acceleration in 1992–2005 due to the extrapolation of the TVG part at this time span.

For the Jason-2 time span (2008–2019), most models tested show a comparable performance, though CNES RL04 and RL05 provide smallest mean of the standard deviations of SXO differences.

The RMS values of orbit differences in the radial direction are of 0.7 cm for Jason-3 orbits computed using the latest versions of CNES models, namely CNES RL04MF and RL05MF. Older Earth's gravity field models, such as GRIM5-C1, EIGEN-GL04S1, EIGEN-6S, EIGEN-6S2ext2, and CNES RL03MF, derived using data by 2009–2014, indicate larger RMS values of radial orbit differences of 0.8–1.9 cm. EIGEN-6S and CNES RL04MF models derived using data at the time spans by 2017 show a trend in RMS values of radial orbit differences and increased scatter of these differences.

The results obtained in this study show an importance of regular reprocessing of Earth's gravity field models for POD of Earth orbiting (altimetry) satellites by determining Earth's TVG at the complete time span at which POD is to be performed. Modeling secular and periodic variations of the Earth's gravity is important to get high-quality satellite orbits, especially in times of climate change on the Earth.

Appendix A: POD Setup

The main models used in the POD in this paper are given in Tables 5, 6, 7, 8, and 9.

Table 5 Force models used

Force component	Model description
Earth's gravity field	The models of Table 3,
	static part: up to d/o 120,
	time-variable part: maximum d/o are from the model
Lunar gravitational attraction	Konopliv et al. (2001), up to d/o 50
Third body gravity attraction	Moon, Sun, Mercury, Venus, Mars, Jupiter, Saturn
	(DE 421, Folkner et al. (2008))
Solar radiation pressure	Constant radiation with eclipse modeling
Atmospheric drag	NRLMSISE-00 model (Picone et al. 2002),
	Horizontal Wind Model HWM14 (Drob et al. 2015)
Earth's radiation pressure	Albedo and infrared (Knocke et al. 1988)
Solid Earth tides	IERS Conventions 2010 (Petit and Luzum 2010)
Ocean tides	EOT11A (Savcenko and Bosch 2012) up to d/o 30
	+ 62 admittance waves (Petit and Luzum 2010)
Atmospheric tides	Biancale and Bode 2003 (Biancale and Bode 2006)
General relativistic correction	Schwarzschild, de Sitter, Lense-Thirring
	(Petit and Luzum 2010)
Thermal radiation	Applied[a] for Jason-1/-2/-3
Non-tidal perturbations (atmospheric, oceanic, hydrological)	Not applied

[a](https://ilrs.cddis.eosdis.nasa.gov/docs/Jason-1_specs.pdf)

Table 6 Reference frame

Component	Its description
Terrestrial Reference Frame	SLRF2020 with post-seismic deformations and periodic variations from ITRF2020 (Altamimi et al. 2023)
Inertial reference frame	Geocentric Celestial Reference System (GCRS)
Precession/nutation	IAU2000A/IAU2006 model up to degree 10 (Mathews et al. 2002)
Earth Orientation Parameters	IERS EOP 20 C04[a]
Mean pole	Quadratic mean pole convention for GRIM5-C1, EIGEN-GL04S1 and EIGEN-6S; Linear mean pole for all other gravity field models

[a]http://hpiers.obspm.fr/iers/eop/eopc04/eopc04.1962-now

Table 7 SLR measurement corrections and settings

Component	Its description
Tropospheric zenith correction	Mendes-Pavlis with temperature correction (Mendes and Pavlis 2004)
Tropospheric mapping function	Mendes et al. (2002)
Relativistic range correction	Petit and Luzum (2010)
Center-of-mass correction	Satellite-dependent, available from the IDS satellite mass history files
SLR measurement correction	TOPEX/Poseidon: Zeitlhöfler et al. (2023), Jason-1/-2/-3: none
Range biases	LAGEOS-1 long-term mean range biases from the ILRS Data Handing File for SLRF2020 (version of 13 February 2024)
Time biases	not applied
Elevation cut-off angle	5°
Observation weight	1 cm, no elevation- and station-dependent weighting applied

Table 8 SLR station coordinate corrections

Component	Its description
Station eccentricities	ILRS eccentricity file[a]
Station discontinuities	ILRS discontinuity file[b]
Solid earth tidal correction	Anelastic model (Petit and Luzum 2010)
Permanent tide	Conventional model (Petit and Luzum 2010)
Ocean tide loading	EOT11a (Savcenko and Bosch 2012)
Atmospheric tidal loading	S1/S2 tidal model (Ray and Ponte 2003)
Solid earth pole tide displacement	Secular pole model (Petit and Luzum 2010)
Ocean pole tide loading	Desai (2002)
Non-tidal displacement (atmospheric, oceanic, hydrological)	Not applied

[a]https://cddis.nasa.gov/archive/slr/slrocc/ecc_xyz.snx

[b]ftp://edc.dgfi.tum.de/pub/slr/aux_data/ILRS_Discontinuities_File.snx

Table 9 Satellite information

Component	Its description
Orbit integration step size	30 s
SLR array offset	TOPEX/Poseidon[a], Jason-1[b], Jason-2[c], Jason-3[d]
Satellite mass	Time-variable[e]
Satellite attitude	Nominal yaw steering model for TOPEX/Poseidon[f], measured attitude for Jason-1/-2/-3 available from[g] and preprocessed according to Bloßfeld et al. (2020)
Satellite macromodel	CNES box-wing model (Cerri et al. 2023)

[a]https://ilrs.gsfc.nasa.gov/missions/satellite_missions/past_missions/topx_com.html

[b]https://ilrs.gsfc.nasa.gov/missions/satellite_missions/past_missions/jas1_com.html

[c]https://ilrs.gsfc.nasa.gov/missions/satellite_missions/past_missions/jas2_com.html

[d]https://ilrs.gsfc.nasa.gov/missions/satellite_missions/current_missions/jas3_com.html

[e]ftp://ftp.ids-doris.org/pub/ids/satellites/ja1mass.txt, ftp://ftp.ids-doris.org/pub/ids/satellites/ja2mass.txt, ftp://ftp.ids-doris.org/pub/ids/satellites/ja3mass.txt, ftp://ftp.ids-doris.org/pub/ids/satellites/topmass.txt

[f]ftp://ftp.ids-doris.org/pub/ids/satellites/topatt.txt

[g]https://cddis.nasa.gov/archive/doris/ancillary/quaternions/

Data Availability SLR observations used in this study are freely available from the ILRS. The Earth's gravity field models used in this study are freely available from the ICGEM and provided references.

Code Availability Not applicable.

Materials Availability Not applicable.

Declarations

Conflict of interest The authors declare that they have no conflict of interest.

Ethics Approval and Consent to Participate Not applicable.

Consent for Publication The authors agree on the final version of the paper to be published.

References

Ablain M, Legeais JF, Prandi P, Marcos M, Fenoglio-Marc L, Dieng HB, Benveniste J, Cazenave A (2017) Satellite altimetry-based sea level at global and regional scales. Surv Geophys 38:7–31. https://doi.org/10.1007/s10712-016-9389-8

Altamimi Z, Rebischung P, Collilieux X, Métivier L, Chanard K (2023) ITRF2020: an augmented reference frame refining the modeling of nonlinear station motions. J Geod 97:47. https://doi.org/10.1007/s00190-023-01738-w

Biancale R, Bode A (2006) Mean annual and seasonal atmospheric tide models based on 3-hourly and 6-hourly ECMWF surface pressure data. Scientific Technical Report 06/01, Potsdam: Deutsches Geo-ForschungsZentrum GFZ, 33 p. https://doi.org/10.2312/GFZ.b103-06011. Accessed 17 July 2025

Biancale R, Balmino G, Lemoine J-M, Marty J-C, Moynot B, Barlier F, Exertier P, Laurain O, Gegout P, Schwintzer P, Reigber Ch, Bode A, Gruber T, König R, Massmann F-H, Raimondo JC, Schmidt R, Zhu SY (2000) A new global Earth's gravity field model from satellite orbit perturbations: GRIM5-S1. Geophys Res Lett 27(22):3611–3614. https://doi.org/10.1029/2000GL011721

Bloßfeld M (2015) The key role of Satellite Laser Ranging towards the integrated estimation of geometry, rotation and gravitational field of the Earth. Dissertation, Technische Universität München. http://mediatum.ub.tum.de/doc/1231180/document.pdf Accessed 17 July 2025

Bloßfeld M, Zeitlhöfler J, Rudenko S, Dettmering D (2020) Observation-based attitude realization for accurate Jason satellite orbits and its impact on geodetic and altimetry results. Remote Sens 12(4):682. https://doi.org/10.3390/rs12040682

Bosch W, Dettmering D, Schwatke C (2014) Multi-mission cross-calibration of satellite altimeters: constructing a long-term data record for global and regional sea level change studies. Remote Sens 6(3):2255–2281. https://doi.org/10.3390/rs6032255

Bruinsma SL, Marty JC, Balmino G, Biancale R, Förste C, Abrikosov O, Neumayer H (2010) GOCE gravity field recovery by means of the direct numerical method. In: Lacoste-Francis H (ed.) Proceedings of the ESA Living Planet Symposium, ESA Publication SP-686. ESA/ESTEC. ISBN: 978-92-9221-250-6; ISSN: 1609-042X

Cazenave A, Moreira L (2022) Contemporary sea-level changes from global to local scales: a review. Proc R Soc A 478:20220049. https://doi.org/10.1098/rspa.2022.0049

Cerri L, Lemoine JM, Mercier F, Zelensky NP, Lemoine FG (2013) DORIS-based point mascons for the long term stability of precise orbit solutions. Adv Space Res 52(3):466–476. https://doi.org/10.1016/j.asr.2013.03.023

Cerri L, Couhert A, Ferrage P (2023) DORIS satellites models implemented in POE processing. https://ids-doris.org/documents/BC/satellites/DORISSatelliteModels.pdf Accessed 17 July 2025

Cheng M, Ries J (2023) C20 and C30 variations from SLR for GRACE/GRACE-FO science applications. J Geophys Res Sol Ea 128:e2022JB025459. https://doi.org/10.1029/2022JB025459

CNES 2012. https://grace.obs-mip.fr/variable-models-grace-lageos/mean-fields/release-02/ Accessed 6 June 2025

Couhert A, Cerri L, Legeais J-F, Ablain M, Zelensky NP, Haines BJ, Lemoine FG, Bertiger WI, Desai SD, Otten M (2015) Towards the 1 mm/y stability of the radial orbit error at regional scales. Adv Space Res 55(1):2–23. https://doi.org/10.1016/j.asr.2014.06.041

Data Handling File for SLRF2020, Greenbelt, MD, USA: NASA Crustal Dynamics Data Information System (CDDIS). https://doi.org/10.5067/SLR/slrf_2020_DHF_001. Accessed 10 Oct 2024

Desai SD (2002) Observing the pole tide with satellite altimetry. J Geophys Res 107(C11):3186. https://doi.org/10.1029/2001JC001224

Drinkwater MR, Floberghagen R, Haagmans R, Muzi D, Popescu A (2003) GOCE: ESA's first Earth explorer core mission. In: Beutler G, Drinkwater MR, Rummel R, Von Steiger R (eds.) Earth gravity field from space—from sensors to Earth sciences. Space sciences series of ISSI, vol. 17. Springer, Dordrecht. https://doi.org/10.1007/978-94-017-1333-7_36

Drob DP, Emmert JT, Meriwether JW, Makela JJ, Doornbos E, Conde M, Hernandez G, Noto J, Zawdie KA, McDonald SE, Huba JD, Klenzing JH (2015) An update to the Horizontal Wind Model (HWM): the quiet time thermosphere. Earth Space Sci 2:301–319. https://doi.org/10.1002/2014EA000089

Fecher T, Pail R, Gruber T et al (2017) GOCO05c: a new combined gravity field model based on full normal equations and regionally varying weighting. Surv Geophys 38:571–590. https://doi.org/10.1007/s10712-016-9406-y

Flechtner F, Dahle C, Neumayer KH, König R, Förste C (2010) The Release 04 CHAMP and GRACE EIGEN gravity field models. In: Flechtner F, et al. (ed) System Earth via geodetic-geophysical space techniques. Advanced technologies in Earth sciences. Springer, Berlin, pp 41–58. https://doi.org/10.1007/978-3-642-10228-8_4

Flechtner F, Reigber C, Rummel R, Balmino G (2021) Satellite gravimetry: a review of its realization. Surv Geophys 42:1029–1074. https://doi.org/10.1007/s10712-021-09658-0

Förste C, Flechtner F, Schmidt R, Meyer U, Stubenvoll R, Barthelmes F, König R, Neumayer K-H, Rothacher M, Reigber C, Raimondo J-C, Biancale R (2005) A new high resolution global gravity field model derived from combination of GRACE and CHAMP mission and altimetry/gravimetry surface gravity data. Geophysical Research Abstracts, vol. 7, 04561, 2005, 2nd General Assembly of the European Geosciences Union, Vienna, Austria, 24–29 April, 2005

Förste C, Flechtner F, Stubenvoll R, Rothacher M, Kusche J, Neumayer K-H, König R, Barthelmes F, Raimondo J-C, Biancale R, Bruinsma S, Lemoine JM, Dahle C (2008a) EIGEN-5C—the new GeoForschungsZentrum Potsdam/Group de Recherche de Geodesie Spatiale combined gravity field model. Eos, Transactions, American Geophysical Union, Suppl., 89, 53, AGU 2008 Fall Meeting, San Francisco, 15–19 December, 2008

Förste C, Schmidt R, Stubenvoll R, Flechtner F, Meyer U, König R, Neumayer H, Biancale R, Lemoine J-M, Bruinsma S, Loyer S, Barthelmes F, Esselborn S (2008b) The GeoForschungsZentrum Potsdam/ Groupe de Recherche de Gèodésie Spatiale satellite-only and combined gravity field models: EIGEN-GL04S1 and EIGEN-GL04C. J Geod 82:331–346. https://doi.org/10.1007/s00190-007-0183-8

Förste C, Bruinsma SL, Shako R, Marty JC, Flechtner F, Abrikosov O, Dahle C, Lemoine JM, Neumayer KH, Biancale R, Barthelmes F, König R, Balmino G (2011) EIGEN-6 - A new combined global gravity field model including GOCE data from the collaboration of GFZ-Potsdam and GRGS-Toulouse, Geophysical Research Abstracts, vol. 13, EGU2011-3242-2

Förste C, Bruinsma S, Flechtner F, Marty J-C, Dahle C, Abrykosov O, Lemoine J-M, Neumayer K-H, Barthelmes F, Biancale R, König R, (2013) EIGEN-6C2—a new combined global gravity field model including GOCE data up to degree and order 1949 of GFZ Potsdam and GRGS Toulouse, Geophysical Research Abstracts, vol. 15, EGU2013-4077-1, General Assembly European Geosciences Union. Austria, Vienna, 2013

Förste C, Bruinsma SL, Rudenko S, Abrikosov O, Lemoine J-M, Marty J-C, Neumayer KH, Biancale R (2016) EIGEN-6S4 A time-variable satellite-only gravity field model to d/o 300 based on LAGEOS, GRACE and GOCE data from the collaboration of GFZ Potsdam and GRGS Toulouse, GFZ Data Services. https://doi.org/10.5880/icgem.2016.008

Folkner WM, Williams JG, Boggs DH (2008) The Planetary and Lunar Ephemeris DE 421. Jet Propulsion Laboratory, California Institute of Technology, Memorandum IOM 343R-08-003. ftp://ssd.jpl.nasa.gov/pub/eph/planets/ioms/de421.iom.v1.pdf. Accessed 18 Oct 2024

Gerstl M (1997) Parameterschätzung in DOGS-OC. In: DGFI Interner Bericht, MG/01/1996/DGFI, 2nd edn (in German)

Gruber C, Rudenko S, Groh A, Ampatzidis D, Fagiolini E (2018) Earth's surface mass transport derived from GRACE, evaluated by GPS, ICESat, hydrological modeling and altimetry satellite orbits. Earth Surf Dynam 6:1203–1218. https://doi.org/10.5194/esurf-6-1203-2018

Gruber T, Bode A, Reigber Ch, Schwintzer P, Biancale R, Balmino G, Lemoine J-M (2000) GRIM5-C1: combination solution of the global gravity field to degree and order 120. Geophys Res Lett 27(24):4005–4008. https://doi.org/10.1029/2000GL011589

Hamlington BD, Bellas-Manley A, Willis JK, Fournier S, Vinogradova N, Nerem RS, Piecuch CG, Thompson PR, Kopp R (2024) The rate of global sea level rise doubled during the past three decades. Commun Earth Environ 5:601. https://doi.org/10.1038/s43247-024-01761-5

Ince ES, Barthelmes F, Reißland S, Elger K, Förste C, Flechtner F, Schuh H (2019) ICGEM—15 years of successful collection and distribution of global gravitational models, associated services, and future plans. Earth Syst Sci Data 11:647–674. https://doi.org/10.5194/essd-11-647-2019

International Altimetry Team (2021) Altimetry for the future: building on 25 years of progress. Adv Space Res 68(2):319–363. https://doi.org/10.1016/j.asr.2021.01.022

Jäggi A, Beutler G, Meyer U, Prange L, Bock H, Dach R, Mervart L (2011) Gravity field determination at AIUB: from CHAMP and GRACE to GOCE. EGU General Assembly 2011, Vienna, Austria, 3–8 April 2011

Jolly GW, Moore P (1995) Accuracy assessment of TOPEX/Poseidon dual crossover correction of ERS-1 altimetry. Adv Space Res 16(12):115–118. https://doi.org/10.1016/0273-1177(95)98793-N

Klokočník J, Wagner CA (1999) Combinations of satellite crossovers to study orbit and residual errors in altimetry. Celest Mech Dyn Astr 74:231–242. https://doi.org/10.1023/A:1008397202151

Klokočník J, Kostelecký J, Wagner C, Schwintzer P, Förste Ch, Scharroo R (2004) Evaluation of the accuracy of the EIGEN-1S and -2 CHAMP-derived gravity field models by satellite crossover altimetry. J Geod 78:405–417. https://doi.org/10.1007/s00190-004-0403-4

Knocke P, Ries J, Tapley B (1988) Earth radiation pressure effects on satellites. In: Astrodynamics conference. American Institute of Aeronautics and Astronautics, Reston, Virigina, p. 3. https://doi.org/10.2514/6.1988-4292

Konopliv AS, Asmar SW, Carranza E, Sjogren WL, Yuan DN (2001) Recent gravity models as a result of the Lunar Prospector Mission. Icarus 150(1):1–18. https://doi.org/10.1006/icar.2000.6573

Kvas A, Behzadpour S, Ellmer M, Klinger B, Strasser S, Zehentner N, Mayer-Gürr T (2019) ITSG-Grace2018: overview and evaluation of a new GRACE-only gravity field time series. J Geophys Res Sol Ea 124:9332–9344. https://doi.org/10.1029/2019JB017415

Kvas A, Brockmann JM, Krauss S, Schubert T, Gruber T, Meyer U, Mayer-Gürr T, Schuh W-D, Jäggi A, Pail R (2021) GOCO06s—a satellite-only global gravity field model. Earth Syst Sci Data 13:99–118. https://doi.org/10.5194/essd-13-99-2021

Labroue S, Boy F, Picot N, Urvoy M, Ablain M (2012) First quality assessment of the Cryosat-2 altimetric system over ocean. Adv Space Res 50(8):1030–1045. https://doi.org/10.1016/j.asr.2011.11.018

Landerer FW, Flechtner FM, Save H, Webb FH, Bandikova T, Bertiger WI et al (2020) Extending the global mass change data record: GRACE Follow-On instrument and science data performance. Geophys Res Lett 47:e2020GL088306. https://doi.org/10.1029/2020GL088306

Legeais J-F, Ablain M, Zawadzki L, Zuo H, Johannessen JA, Scharffenberg MG, Fenoglio-Marc L, Fernandes MJ, Andersen OB, Rudenko S, Cipollini P, Quartly GD, Passaro M, Cazenave A, Benveniste J (2018) An improved and homogeneous altimeter sea level record from the ESA Climate Change Initiative. Earth Syst Sci Data 10:281–301. https://doi.org/10.5194/essd-10-281-2018

Lemoine J-M, Bruinsma S, Loyer S, Biancale R, Marty J-C, Perosanz F, Balmino G (2007) Temporal gravity field models inferred from GRACE data. Adv Space Res 39(10):1620–1629. https://doi.org/10.1016/j.asr.2007.03.062

Lemoine JM, Bruinsma S, Gégout P, Biancale R, Bourgogne S (2014) EIGEN-GRGS.RL03.MEANFIELD: new mean gravity field model for altimetric satellite orbit computation, OSTST, Lake Constance, Germany, 27-31.10.2014. https://ostst.aviso.altimetry.fr/fileadmin/user_upload/tx_ausyclsseminar/files/29Ball0900-6_POD_2014_JMLemoine.pdf. Accessed 19 Nov 2024

Lemoine J-M, Bourgogne S, Biancale R, Reinquin F (2018) The new time-variable gravity field model for POD of altimetric satellites based on GRACE+SLR RL04 from CNES/GRGS. IDS Workshop, 24–29.09.2018, Ponta Delgada, Portugal. https://ids-doris.org/images/documents/report/ids_workshop_2018/IDS18_s_LemoineJM_NewtimeVariableGravityFieldModelForPOD.pdf. Accessed 17 July 2025

Lemoine J-M, Bourgogne S, Capdeville H, Reinquin F (2023) New mean gravity field model CNES_GRGS.RL05MF_combined_GRACE_SLR_DORIS, IDS AWG meeting, online, 18.04.2023, https://ids-doris.org/images/documents/report/AWG202304/IDSAWG202304-LemoineJM-NewMeanGravityModel.pdf Accessed 17 July 2025

Mayer-Gürr T, Zehentner N, Klinger B, Kvas A (2014) ITSG-Grace2014: a new GRACE gravity field release computed in Graz. GRACE Science Team Meeting 2014, Potsdam, Germany, 29 September 2014—1 October 2014. http://dx.doi.org/10.13140/RG.2.1.5098.2805

Mayer-Gürr T, Pail R, Gruber T, Fecher T, Rexer M, Schuh W-D, Kusche J, Brockmann J-M, Rieser D, Zehentner N, Kvas A, Klinger B, Baur O, Höck E, Krauss S, Jäggi A (2015) The combined satellite gravity field model GOCO05s. Geophysical Research Abstracts, vol. 17, EGU2015-12364, EGU General Assembly 2015, Vienna, Austria

Mathews PM, Herring TA, Buffett BA (2002) Modeling of nutation and precession: new nutation series for nonrigid Earth and insights into the Earth's interior. J Geophys Res. https://doi.org/10.1029/2001JB000390

Mendes VB, Pavlis EC (2004) High-accuracy zenith delay prediction at optical wavelengths. Geophys Res Lett 31:L14602. https://doi.org/10.1029/2004GL020308

Mendes V, Prates G, Pavlis EC, Pavlis DE, Langley RB (2002) Improved mapping functions for atmospheric refraction correction in SLR. Geophys Res Lett 29(10). https://doi.org/10.1029/2001GL014394

Meyssignac B, Ablain M, Guérou A, Prandi P, Barnoud A, Blazquez A, Fourest S, Rousseau V, Bonnefond P, Cazenave A, Chenal J, Dibarboure G, Donlon C, Benveniste J, Sylvestre-Baron A, Vinogradova N (2023) How accurate is accurate enough for measuring sea-level rise and variability. Nat Clim Chang 13:796–803. https://doi.org/10.1038/s41558-023-01735-z

Ollivier A, Faugere Y, Picot N, Ablain M, Femenias P, Benveniste J (2012) Envisat ocean altimeter becoming relevant for mean sea level trend studies. Mar Geodesy 35:118–136. https://doi.org/10.1080/01490419.2012.721632

Pavlis E, Luceri V (2022) The ILRS contribution to ITRF2020. https://itrf.ign.fr/docs/solutions/itrf2020/The_ILRS_contribution_to_ITRF2020_description_2022.09.23.pdf. Accessed 10 Oct 2024

Pearlman MR, Noll CE, Pavlis EC, Lemoine FG, Combrink L, Degnan JJ, Kirchner G, Schreiber U (2019) The ILRS: approaching 20 years and planning for the future. J Geod 93:2161–2180. https://doi.org/10.1007/s00190-019-01241-1

Peter H, Meyer U, Lasser M, Jäggi A (2022) COST-G gravity field models for precise orbit determination of Low Earth Orbiting Satellites. Adv Space Res 69(12):4155–4168. https://doi.org/10.1016/j.asr.2022.04.005

Petit G, Luzum B (2010) IERS Conventions (2010): IERS Technical Note 36, Working Version 1.3.0. Frankfurt am Main: Verlag des Bundesamts für Kartographie und Geodäsie

Picone JM, Hedin AE, Drob DP, Aikin AC (2002) NRLMSISE-00 empirical model of the atmosphere: statistical comparisons and scientific issues. J Geophys Res 107(A12):1468. https://doi.org/10.1029/2002JA009430

Prandi P, Philipps S, Pignot V, Picot N (2015) SARAL/AltiKa global statistical assessment and cross-calibration with Jason-2. Mar Geodesy 38(sup1):297–312. https://doi.org/10.1080/01490419.2014.995840

Prandi P, Meyssignac B, Ablain M, Spada G, Ribes A, Benveniste J (2021) Local sea level trends, accelerations and uncertainties over 1993–2019. Sci Data 8:1. https://doi.org/10.1038/s41597-020-00786-7

Ray RD, Ponte RM (2003) Barometric tides from ECMWF operational analyses. Ann Geophys 21:1897–1910. https://doi.org/10.5194/angeo-21-1897-2003

Reigber Ch, Balmino G, Schwintzer P, Biancale R, Bode A, Lemoine J-M, König R, Loyer S, Neumayer H, Marty J-C, Barthelmes F, Perosanz F, Zhu SY (2002) A high quality global gravity field model from CHAMP GPS tracking data and accelerometry (EIGEN-1S). Geophys Res Lett 29(14):1692. https://doi.org/10.1029/2002GL015064

Reigber C, Lühr H, Schwintzer P (Eds) (2003) First CHAMP mission results for gravity, magnetic and atmospheric studies. Springer, Berlin. https://doi.org/10.1007/978-3-540-38366-6

Reigber Ch, Jochmann H, Wünsch J, Petrovic S, Schwintzer P, Barthelmes F, Neumayer K-H, König R, Förste Ch, Balmino G, Biancale R, Lemoine J-M, Loyer S, Perosanz F (2005a) Earth Gravity Field and Seasonal Variability from CHAMP. In: Reigber C, Lühr H, Schwintzer P, Wickert J (eds) Earth Observation with CHAMP. Springer, Berlin. https://doi.org/10.1007/3-540-26800-6_4

Reigber Ch, Schmidt R, Flechtner F, König R, Meyer U, Neumayer K-H, Schwintzer P, Zhu SY (2005b) An Earth gravity field model complete to degree and order 150 from GRACE: EIGEN-GRACE02S. J Geodyn 39(1):1–10. https://doi.org/10.1016/j.jog.2004.07.001

Reigber C, Schwintzer P, Stubenvoll R, Schmidt R, Flechtner F, Meyer U, König R, Neumayer K-H, Förste C, Barthelmes F, Zhu SY, Balmino G, Biancale R, Lemoine J-M, Meixner H, Raimondo J-C (2006) A high resolution global gravity field model combining CHAMP and GRACE satellite mission and surface data: EIGEN-CG01C. Scientific Technical Report STR, 06/07, Potsdam, Deutsches Geo-ForschungsZentrum GFZ, 12 p. https://doi.org/10.2312/GFZ.b103-06075

Rosborough GW (1986) Satellite orbit perturbations due to the geopotential, Report CSR-86-1, Center for Space Research, University of Texas, Austin, USA. http://dx.doi.org/10.26153/tsw/12697

Rudenko S, Dettmering D, Esselborn S, Schöne T, Förste C, Lemoine J-M, Ablain M, Alexandre D, Neumayer K-H (2014) Influence of time variable geopotential models on precise orbits of altimetry satellites, global and regional mean sea level trends. Adv Space Res 54(1):92–118. https://doi.org/10.1016/j.asr.2014.03.010

Rudenko S, Bloßfeld M, Müller H, Dettmering D, Angermann D, Seitz M (2018) Evaluation of DTRF2014, ITRF2014, and JTRF2014 by precise orbit determination of SLR Satellites. IEEE Trans Geosci Remote 56(6):3148–3158. https://doi.org/10.1109/TGRS.2018.2793358

Rudenko S, Esselborn S, Schöne T, Dettmering D (2019) Impact of terrestrial reference frame realizations on altimetry satellite orbit quality and global and regional sea level trends: a switch from ITRF2008 to ITRF2014. Solid Earth 10(1):293–305. https://doi.org/10.5194/se-10-293-2019

Rudenko S, Dettmering D, Zeitlhöfler J, Alkahal R, Upadhyay D, Bloßfeld M (2023) Radial orbit errors of contemporary altimetry satellite orbits. Surv Geophys 44:705–737. https://doi.org/10.1007/s10712-022-09758-5

Rudenko S, Bloßfeld M, Kehm A, Dettmering D, Zeitlhöfler J (2025) Impact of SLR long-term mean range biases on SLRF2020-based orbits of altimetry satellites. Earth Planets Space 77:59. https://doi.org/10.1186/s40623-025-02183-z

Sandford C, Dunn R, Titchner H, Kendon M, Rayner N, Morice C, Palmer M, McCarthy M, Kaye N (2024) Global and regional climate in 2023. Weather. https://doi.org/10.1002/wea.7636

Savcenko R, Bosch W (2012) EOT11A—Empirical Ocean Tide model from multi-mission satellite altimetry. Deutsches Geodätisches Forschungsinstitut der Technische Universität München (DGFI-TUM), Munich, Report no. 89, 49 pp. https://hdl.handle.net/10013/epic.43894.d001 Accessed 17 July 2025

Schrama EJO, Visser PNAM (2024) Choices for temporal gravity field modeling for precision orbit determination of CryoSat-2. Adv Space Res 73(1):31–41. https://doi.org/10.1016/j.asr.2023.11.034

Shako R, Förste C, Abrykosov O, Bruinsma S, Marty J-C, Lemoine J-M, Flechtner F, Neumayer K-H, Dahle C (2014) EIGEN-6C: a high-resolution global gravity combination model including GOCE data. In: Flechtner F, Sneeuw N, Schuh WD (Eds) Observation of the system Earth from space—CHAMP,

GRACE, GOCE and future missions. Advanced Technologies in Earth Sciences. Springer, Berlin. https://doi.org/10.1007/978-3-642-32135-1_20

Tapley BD, Chambers DP, Cheng MK, Kim MC, Poole SR, Ries JC (2000) The TEG-4 Earth gravity field model. Paper presented at the XXV General Assembly of the European Geophysical Society, Nice, France, 27 April 2000

Tapley BD, Bettadpur S, Watkins M, Reigber C (2004) The gravity recovery and climate experiment: mission overview and early results. Geophys Res Lett 31:L09607. https://doi.org/10.1029/2004GL019920

Tapley B, Ries J, Bettadpur S, Chambers D, Cheng M, Condi F, Gunter B, Kang Z, Nagel P, Pastor R, Pekker T, Poole S, Wang F (2005) GGM02—an improved Earth gravity field model from GRACE. J Geod 79:467–478. https://doi.org/10.1007/s00190-005-0480-z

The 2022 GCOS ECVs Requirements (GCOS 245), World Meteorological Organization, 2022. https://ocean rep.geomar.de/id/eprint/57694/1/GCOS-245_2022_GCOS_ECVs_Requirements.pdf Accessed 17 July 2025

Weigelt M, Jäggi A, Meyer U, Arnold D, Mayer-Gürr T, Öhlinger F, Sośnica K, Ebadi S, Schön S, Steffen H (2024) Bridging the gap between GRACE and GRACE Follow-On by combining high–low satellite-to-satellite tracking data and satellite laser ranging. J Geod 98:84. https://doi.org/10.1007/s00190-024-01888-5

World Meteorological Organization State of the Global Climate 2023. https://library.wmo.int/records/item/68835-state-of-the-global-climate-2023 Accessed 17 July 2025

Yi S, Sneeuw N (2021) Filling the data gaps within GRACE missions using Singular Spectrum Analysis. J Geophys Res Sol Ea 126:e2020JB021227. https://doi.org/10.1029/2020JB021227

Zeitlhöfler J, Bloßfeld M, Rudenko S, Dettmering D, Seitz F (2023) Station-dependent satellite laser ranging measurement corrections for TOPEX/Poseidon. Adv Space Res 71(1):975–996. https://doi.org/10.1016/j.asr.2022.09.002

Zelensky NP, Lemoine FG, Beckley BD, Chinn DS, Pavlis DE (2018) Impact of ITRS 2014 realizations on altimeter satellite precise orbit determination. Adv Space Res 61(1):45–73. https://doi.org/10.1016/j.asr.2017.07.044

Publisher's Note Springer Nature remains neutral with regard to jurisdictional claims in published maps and institutional affiliations.

Authors and Affiliations

Sergei Rudenko[1,2] · **Denise Dettmering[1]** · **Jean-Michel Lemoine[3]** · **Mathis Bloßfeld[1]** · **Julian Zeitlhöfler[1]**

✉ Sergei Rudenko
sergiy.rudenko@kit.edu

Denise Dettmering
denise.dettmering@tum.de

Jean-Michel Lemoine
Jean-Michel.Lemoine@cnes.fr

Mathis Bloßfeld
mathis.blossfeld@tum.de

Julian Zeitlhöfler
julian.zeitlhoefler@tum.de

[1] Deutsches Geodätisches Forschungsinstitut (DGFI-TUM), Technical University of Munich, Arcisstraße 21, 80333 Munich, Germany

[2] Present Address: Geodetic Institute, Karlsruhe Institute of Technology (KIT), Kaiserstraße 14, 76131 Karlsruhe, Germany

[3] DTN/CD/GS BPI 3100, Centre National d'Etudes Spatiales (CNES), 18 avenue Edouard Belin, 31401 Toulouse, France